Author's response

The reviewers' comments are written in blue and bold. The corresponding responses and changes in the manuscript are written in black.

Anonymous referee # 1
General comment (1)

1. **It would be easier for the reader if all figures representing the same regions were all placed in the same order, e.g. as seen in Fig. 2 and keep the same regions in all other figures. For example, in Fig.2 SA branches (L, R1, R2, R3) are in the far right panels, while in Fig. 3 they are in far left panels and in Fig.4 they are in the middle. It may be a detail, but it would help uniformity and help the reader.**

Response: The order of figures has been corrected and kept the same throughout the manuscript.

Changes in the manuscript: The order of figures in Figures 3 and 4, and their titles have been modified for uniformity.

Specific comments (2-8)

2. **The standard deviation of κ (σ(κ)) around κ is often used as an estimate of the degree of heterogeneity (chemical dispersion) of particles (Psichoudaki et al., 2018; Lance et al., 2013). This could further be associated with the diurnal variability in the observed activation fractions as well as the chemical composition.**

Response: We appreciate that this analysis was pointed out. Figure 1shows the diurnal variation of chemical dispersion for the various air-masses. The chemical dispersion analysis has been explained below.

"At this junction, it would also be pertinent to mention how chemical dispersion and parameters governing CCN are inter-connected. The standard deviation of κ (σ(κ)) around κ is often used as an estimate of the degree of heterogeneity (chemical dispersion) of particles (Psichoudaki et al., 2018; Lance et al., 2013). The chemical dispersion for all air masses and their sub-branches have been shown in Figures 6, S4 and S5. The chemical dispersion for SA air mass during the early hours (6:00-8:00) coincided with chloride emissions and during the late night after 20:00 with POA and OOA emissions. During the time of high chloride emissions, κ also peaked since inorganics are associated with high hygroscopicity, while during the late hours, κ dropped due to an increase in organics associated with low hygroscopcity. The diurnal patterns of activated fraction, GMD and chemical dispersion were also similar. This implies that higher heterogeneity shifts GMD to a high value, thereby increasing the available regime for activation and vice-versa. There was no discernible pattern noted for the other air masses."

Figure1: Diurnal variation of chemical dispersion for the various air masses (a) AS, BB and SA, (b) B and B.reg, and, (c) L, R1, R2 and, R3.
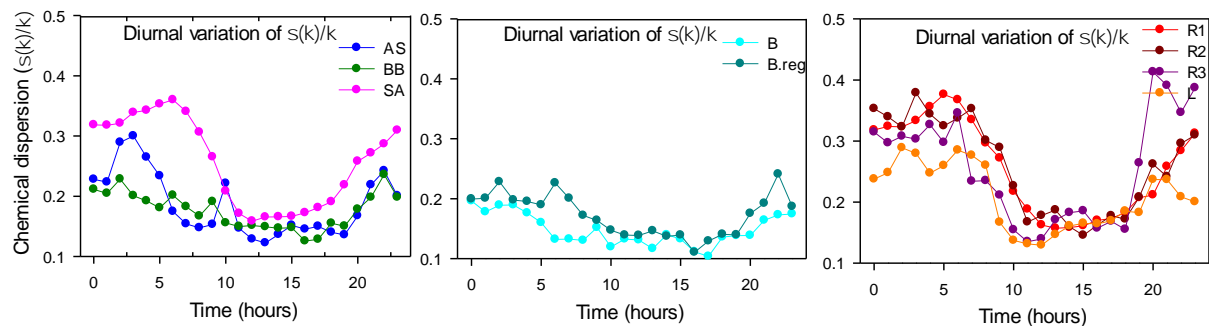
Changes in the manuscript: The above text has been added to the manuscript at P18, L26-30 and P19, L1-5. The references, Psichoudaki et al., 2018 and Lance et al., 2013 have been added to the list of references. Figure 1(a) has been included as Figure 6(e), while Figures 1(b) and 1(c) have been included in the Supplement as Figures S4 and S5 respectively. The figure captions have also been amended accordingly.

3. Since an AE33 aethalometer was used, the contribution of BCwb can be estimated (e.g. Sandradewi et al. 2008) in order to further verify the presence of biomass burning aerosol in the SA branches (P11,L7-8 and elsewhere (e.g. P11,L20-21)). The second component (BCff) could also verify traffic emissions (e.g. P13, L8-11).

Response: We are thankful for pointing out this analysis. Table 1 shows the contribution of BCwb and BC ff for the various air masses. The detailed explanation has been presented below in Text 1 and Text 2.

Text 1:

"In order to determine the presence of biomass burning and traffic emissions, BCwb (wood-burning component) and BCff (traffic component) for all air masses were determined based on Aethalometer data as per Sandradewi et al. 2008. The contribution of BCwb and BCff have been summarized in Table S4. Since fossil fuel sources are active the year-round, there is a strong presence of BCff ranging from 70% to 86%. However, biomass burning is only active during certain specific times for short durations and is very prominent in the north-west direction for the SA air masses. It was observed that the more distant air masses exhibited a higher BCwb contribution compared to those originating within close proximity. Hence, while L was associated with 13.9% BCwb, R3 exhibited 29.2% BCwb. The BCwb contribution for A and BB air masses was 21%. It can thus be concluded that both biomass burning and traffic emissions are important sources contributing to the chemical composition of the various air masses."

Text 2:

"As far as the increase in chloride with the increasing length of trajectories is concerned, the most plausible explanation is biomass burning. It has been pointed out in Section 3.2 earlier that BCwb contribution increases as the air mass trajectories become distant, a feature similar to chloride emissions."

Table1: Contribution of BCwb and BCff for the various air masses

Cluster	BCwb	BCff

A	21%	79%
BB	21.60%	78.40%
SA	24.70%	75.30%
B	26.80%	73.20%
B.reg	21.60%	78.40%
L	13.90%	86.10%
R1	25.20%	74.80%
R2	29%	71%
R3	29.20%	70.80%

Changes in the manuscript: Text 1 has been added to the manuscript at P9, L26-29 and P10, L1-6. Text 2 has been added to the manuscript at P10, L22-24. The reference Sandradewi et al. 2008 has been added to the list of references. Table 1has been included in the Supplement as table S4. The table caption has been added to the list of Tables in the manuscript.

3. **P2,L1-3: High activation fractions as high as 0.8% at 0.38% SS have been observed at the eastern Mediterranean for air masses originating from the South (Bougiatioti et al., 2009)**

Response: This statement was made with reference to continental locations. Accordingly, the referred text has been edited as under:

"The a_f was governed mainly by the Geometric Mean Diameter (GMD), and such a high a_f (0.71±0.14 for the most dominant sub-branch of SA air mass (R1) at 0.4% SS) has not been seen anywhere in the world for a continental site."

Changes in the manuscript: The above text has been added to the manuscript at P2, L1-3.

4. **Fig.3 BB (middle panels) for BC: it seems that many points are missing in the diurnal variability for B region, which is not commented in the text (P11,L20-28, P12,L21-28). Why is that?**

Response: Unfortunately, the Aethalometer was not working during that time period and hence BC data could not be collected. The unavailability of data for BC for B region has now been pointed out with the addition of the following text:

"The missing points in the diurnal variability of BC for B region are on account of unavailability of Aethalometer data."

Changes in the manuscript: The above text has been added at P13, L 9-10.

5. **P14, L14-15: Also for the city of Athens, Greece, during wintertime when biomass burning is an important source of organic aerosol, overall hygroscopicity parameter ranged from 0.15 to 0.25 with lower values (around 0.16) being observed during night when biomass burning particles prevailed (Psichoudaki et al., 2018).**

Response: The above comment has been included.

Changes in the manuscript: The text at P14, L26-28 now reads as under:

"κ has also been found to vary from 0.15 to 0.25 with lower values (around 0.16) being observed during night when biomass burning particles prevailed during wintertime at Athens, Greece (Psichoudaki et al., 2018). Thus, κ values for Delhi can represent both secondary formation and biomass burning."

6. **P3,L7 Detailed CCN and _ measurements have been carried out (delete "in India") .**

Response: The term "in India" has been deleted.

Changes in the manuscript: The term "in India" has been deleted from the text at P3, L9.

7. **Fig.2 (c) should read PM1 species, as now it is identical to (a)**

Response: Fig.2(c) has been corrected to read PM1 species.

Changes in the manuscript: Fig.2(c) caption has been changed to "PM1 species".

Anonymous referee # 2

General comments (1-2)

1. **At the moment there is no evaluation of the quality of the data since there was no independent PM1measurement or CCN counter. But something can be done. A straightforward way would be to make a closure study of mass calculated from the number size distributions measured with the SMPS and as the sum of the chemical constituents of the ACSM + BC. Doing that remember the SMPS shows size distributions using mobility diameters whereas the ACSM size range is with aerodynamic diameters. I would like to see scatter plots for the major air masses and some discussion on them.**

Response: This analysis is indeed important. However, it has already been covered in a parallel manuscript Gani et al. 2019 that addresses the DAS (Delhi Aerosol Supersite) campaign. The relevant scatter plot for mass closure has also been shown in the supplement (Figure S1). The following excerpt taken from Gani et al. 2019 addresses the above comment:

"*Using speciated mass concentrations and the PSD, we observed that C-PM$_1$ was highly correlated with SMPS-PM$_1$ (R^2=0.83), and we achieved almost complete mass closure (Fig. S1). That most of the PM$_1$ was composed of nonrefractory material and BC was consistent with past literature from Delhi which observed that metals and other nonrefractory crustal materials, which we did not measure in this study, constituted less than 5 % of PM$_1$ (Jaiprakash et al., 2017). We estimated that the C-PM$_1$ concentrations observed at our site were generally ~85 % of the PM$_{2.5}$ concentrations (R^2=0.54 and slope=0.85 for linear fit of hourly C-PM$_1$ and PM$_{2.5}$ concentrations over entire campaign) measured at the nearest monitoring station that is operated by the Delhi Pollution Control Committee (DPCC), R.K. Puram (3 km away), where the annual average PM$_{2.5}$ concentration for 2017 was 140 μg m^{-3}.*"

Changes in the manuscript: The following text has been added to P8, L13-14:

"Mass closure between SMPS size distribution data and sum of ACSM species together with BC was achieved ($R^2=$ 0.83) as detailed in our parallel manuscript Gani et al. 2019."

2. **Another thing that I noticed is that the hygroscopicity parameter was calculated using only ACSM data. There was a lot of BC in air and that definitely as also an effect on κ. Find κ (BC) from the literature and repeat the calculations taking also BC into account.**

Response: The impact of BC on κ has been detailed below:

Text 1:

"κ for BC has been taken as zero in several studies in the past (Hong et al., 2014, Leng et al., 2014, Wu et al., 2013)."

Text 2:

"Including BC in κ calculations leads to a difference of 10% in κ on an average, shifting the mean κ of 0.32 to 0.29. The BC mass fraction and volume fraction were 10% and 9% respectively. Thus, change in κ due to introduction of BC was not significant."

Changes in the manuscript: Text 1 has been added at P5, L22-23. Text 2 has been added to P14, L12-15. The references, Hong et al., 2014, Leng et al., 2014, Wu et al., 2013 have been added to the list of references.

Detailed comments (3-27)

3. **P1,L12-13 The first sentence of the abstract "This work presents for the first time long term and time-resolved estimates of hygroscopicity parameter (κ) and CCN for Delhi" emphasizes that the measurements were long term. That is not really true since in generally long-term measurements are such that also trends of various properties can be estimated. A bit more than one year of data cannot be considered long term. Another thing is that the paper mainly presents variations of chemical composition, only a small part is about CCN. So it is somewhat misleading to start the abstract with the κ and CCN.**

Response: With reference to CCN and κ estimates, such studies are usually short term and span over a month. This data is hence huge as it spans for more than a year. The term "long term" has been replaced by "spanning for more than a year". In addition to it, the paper presents variations of chemical properties but it has been tried best to capture their effects on both κ and CCN. The aim of starting the abstract with this idea is because this is the most valuable contribution of the work and is extremely relevant for the Indian sub-continent that faces a dearth of such data.

The first sentence of the abstract has been modified as:

"Delhi is a megacity that is subjected to high local anthropogenic emissions and long-range transport of pollutants. This work presents for the first time time-resolved estimates of hygroscopicty parameter (κ) and CCN spanning for more than a year derived from chemical composition and size distribution data."

Changes in the manuscript: The text within quotes has been added to P1, L12-14.

4. **P3,L31-32 "... relatively lesser traffic compared to the city in general ..."**

Response: The word "lesser" has been replaced by "less".

Changes in the manuscript: The word "lesser" has been replaced by "less" at P3, L33 and all its occurrences in the manuscript.

5. **P3, Section 2.1 This is the section showing the ACSM instrument. Write the particle size range it measures.**

Response: It has been mentioned in Section 2.1 that ACSM is equipped with a PM1 cyclone.

Changes in the manuscript: None

6. **P4, L13 in the title 2.2, is the acronym OOA right or should it be POA?**

Response: It should be OOA as the speciation of organics has been discussed.

Changes in the manuscript: None

7. **P4, L31 What are the residuals here? Explain.**

Response: "Residuals represent the deviation of the cluster means from the reference profiles." The mathematical definitions have been given in Equations 1 and 2in the manuscript.

Changes in the manuscript: The text below has been added at P4, L32-33.

"This was followed by evaluation of residuals. Residuals represent the deviation of the cluster means from the reference profiles."

8. **P5,L6-17 This text looks like it is taken from a computer program. Explain in a short text the contents of it and move this text to the supplement.**

Response: The referred text has been replaced with the following text:

Text 1:

"The residuals of the cluster means were then compared with the reference residuals as per six conditions described in detail in Text S1 and classified as HOA, BBOA, OOA or mixed."

Changes in the manuscript: Text 1 above has been added to P5, L9-10. The remaining text has been moved to the supplement.

9. **P5,L24-26. Present the hygroscopicity parameters of the different compounds clearly in a table and add there the references of the papers where you got them from. A compilation like that helps the readers.P5,L32 Bhattu et al. (2015) calculated Dc using ammonium sulfate, ammonium nitrate, insoluble organics and soluble organics and gives the respective constants. You have different constituents so you should show all constants you have used either in a table or in the text like Bhattu et al. (2015) did.**

Response: This has been addressed by the addition of the following text:

"κ_i values were taken as 0.61 for $(NH_4)_2SO_4$, 1.02 for NH_4Cl and 0.67 for NH_4NO_3 (Sullivan et al., 2009; Petters and Kredenweis 2007). The density values to estimate the volume fraction of the inorganic constituents were taken as 1770kg m^{-3} for $(NH_4)_2SO_4$, 1519 kg m^{-3} for NH_4Cl and 1720 kgm^{-3} for NH_4NO_3 (CRC Handbook of Physics and Chemistry, 95th Edition). The density of organics was taken as 1500 kg m^{-3} (Bougiatioti et al., 2009)."

The hygroscopicity parameter for organics has already been reported in the manuscript.

Changes in the manuscript: The text within quotes above has been added to P5, L18-22. The references, Sullivan et al., 2009, Petters and Kredenweis, 2007, for CRC Handbook of Physics and Chemistry, 95th Edition and Bougiatioti et al., 2009have been added to the list of references.

10. P6,L1, "...CCN.." -> NCCN

Response: CCN has been replaced by 'NCCN'.

Changes in the manuscript: At P5, L31 CCN has been replaced by "N_{CCN}".

11. P6, Eq (4) correct toulene -> toluene

Response: *The word 'toulene' has been corrected to 'toluene'.*

Changes in the manuscript: The above spelling correction has been made to Eq. 4 and text at P6, L28-29.

12. P7,L1 [OH] is definitely not constant, it varies a lot. Discuss this a bit.

Response: The value for OH has been taken as 1.5×10^6 molecules cm^{-3} for aging calculations similar to Nault et al. 2018 for aging calculations. We agree that [OH] is not constant, however, assuming it to be constant for aging calculations is standard practice (Nault et al. 2018). As per the authors' knowledge, the detailed diurnal variation of [OH] for Delhi is not known and hence has not been commented upon.

Changes in the manuscript: The following text has been added to the manuscript at P6, L30 and P7, L1-2.

"The [OH] concentration is not constant and varies considerably temporally and spatially, but due to unavailability of data pertaining to its variation for Delhi, it has been assumed constant for aging calculation."

13. P8,L19 Define aerosol neutralization ratio. Explain and give formulas.

Response: Aerosol Neutralization Ratio (ANR) is explained below:

"ANR is defined as the normalized ratio of the measured NH_4^+ concentration to the NH_4^+ concentration needed for full neutralization of the anions and calculated as per Eq. (5) (Zhang et al. 2007).

$$\text{ANR} = \frac{NH_4^+ meas}{NH_4^+ neut} = \frac{(NH_4^+/18)}{(2XSO_4^{2-}/96)+(NO_3^-/62)+(Cl^-/35.5)} \qquad (5)"$$

Changes in the manuscript: The above text within quotes has been added to P8, L22-25.

14. P8,L28, 1 < R > 2 is never possible. Correct.

Response: This has been corrected to 1<R<2.

Changes in the manuscript: The correction "$1 < R[SO_4^{2-}] < 2$" has been done at P9, L5.

15. P9,L12 "...AS was associated with BBOA...". What does this mean?

Response: It implies that the organic aerosols for the AS (Arabian Sea) air mass are of biomass burning type.

Changes in the manuscript: The text at P9, L18-20 has been modified as under:

"The organic speciation revealed that AS organics were BBOA, BB organics wherein both B organics and B.reg organics were mixed and SA organics were BBOA wherein L, R1, and R2 organics were BBOA and R3 organics included both HOA and BBOA."

16. P10,L15, "... ammonium nitrate is relatively more stable than ammonium chloride..." Give a reference.

Response: This has been explained in Kaneyasu et al., 1999.

Changes in the manuscript: The reference "Kaneyasu et al., 1999" has been added at P11, L3.

17. P10,L20 "chloride depletion". Give formula or explain clearly what you mean here. I have calculated chloride depletion when comparing Cl-to-Na ratios in filter samples with the same ratios in pure sea salt. Now it is not possible, ACSM gives no Na concentrations.

Response: "Chloride depletion" refers to the decrease in chloride concentrations for SA air mass beginning close to mid-day. This is not with reference to Cl-to-Na ratios. To avoid ambiguity, it has been replaced with the term "reduction in chloride concentrations."

Changes in the manuscript: The term "reduction in chloride concentrations" has been added to P11, L8.

18. P11,L4 "Hike in sulphate concentration...". What does hike mean here? Explain or rewrite clearly.

Response: "Hike in sulphate concentration..." implies a peak or increase in sulphate concentration and the word 'hike' has been replaced by the word 'peak' for clarity.

Changes in the manuscript: All occurrences of 'hike' have been replaced by 'peak' in the manuscript and also at P11, L22 as suggested.

19. P12,L14 "The correlation of NO3 with ns-NH4 was found to be very poor..." Show some scatter plots, eithier in the main text or the supplement.

Response: Thank you for pointing this out. The noise in the data for correlation calculation was not removed for B.reg. For both B and B.reg, ns-NH_4^+ correlated well with NO_3^-, the correlation values being 0.63 and 0.70 respectively.

Figure2: Scatter plots between ns-NH_4^+ vs. NO_3^- for B (left) and B.reg (right) branches.
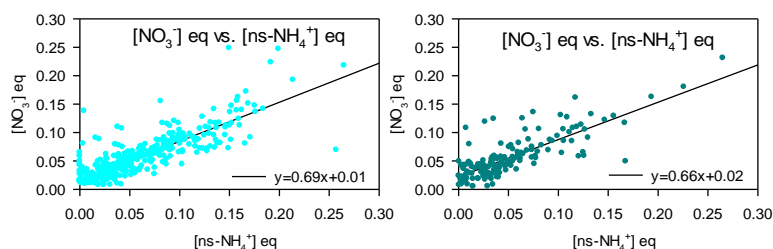
This also resulted in a change in the dominant salt assumption for B.reg, which was earlier only $(NH_4)_2SO_4$. It has been changed to $(NH_4)_2SO_4$ and NH_4NO_3.

Changes in the manuscript: The following changes have been made.

1. P13, L3-L5 has been edited as under:

"The correlation of $[NO_3^-]$ with $[ns-NH_4^+]$ was found to be appreciably high for both B and B.reg. For both of these branches, the fossil fuel combustion resulting in NO_3^- emissions in combination with NH_4^+ (Rajput et al., 2015; Pan et al., 2019) can lead to NH_4NO_3 formation."

2. P9, L13-14 has been edited as under:

"Coupling of $ns-NH_4^+$ with NO_3^- revealed a good correlation for B (0.70) and B.reg (0.63) (Figure S6)."

3. P9, L16-17 has been edited as under:

"Thus, the dominating salts are $(NH_4)_2SO_4$ for AS, $(NH_4)_2SO_4$ and NH_4NO_3 for BB air-mass and NH_4Cl for SA and its sub-branches."

4. The scatter plots in Figure 2 have been included in the supplement as Figure S6.

20. P12,L21 " The BC concentration in BB air masses was considerably lower than SA." Here is a grammatical error. The sentence means that BC concentration is smaller than South Asia! It should be " The BC concentration in BB air masses was considerably lower than in the SA air masses." There are similar errors in several sentences in the paper. Check and correct.

Response: The suggested correction has been considered and taken care of throughout the manuscript.

Changes in the manuscript: P13, L9 has been corrected to "The BC concentration in BB air masses was considerably lower than in the SA air mass". All such errors have been likewise corrected.

21. P13,L5 "lesser" is a wrong word. Rewrite the sentence

Response: The word "lesser" has been replaced by "less".

Changes in the manuscript: "Lesser" has been replaced by "less" at P13, L22 and at all other occurrences in the manuscript.

22. P13,L13 " Both BC and POA are quite less compared to SA." I don't understand, rewrite.

Response: It implies that the BC and POA concentrations for the AS air mass are substantially low relative to their concentrations for the SA air mass. It has been replaced with the text: "Both BC and POA for AS air mass are less than in the SA air mass."

Changes in the manuscript: The quoted text above has been added to P14, L1.

23. P13,L17-24 This text is clearly conclusions so why don't you have it there in the "Conclusions" section?

Response: The referred text partly has been moved to the "Conclusions" section and the remaining part has been retained to interlink with the next section on hygroscopicity.

Changes in the manuscript: The following text has been moved to P19, L19-24 under the "Conclusions" section.

"The high PM1 concentration for Delhi which exceeds the National Ambient Air Quality Standards can be mitigated only by controlling both the primary emissions and precursors. In order to address the situation justly, following measures are lacking: a) Data enlisting measurements of PM_1 emissions from various industries in India and Asia, b) Description of the chemical constituents of aerosol that are being emitted, both qualitatively and quantitatively, c) Defining emission limits and complying with the same."

24. P13, L26 A bit more than a year is not "long term".

Response: This has been discussed in response to 3.

Changes in the manuscript: Same as in response to 3.

25. How do the κ values look like when you take BC into account?

Response: This has been discussed in response to 2.

Changes in the manuscript: Same as in response to 2.

26. P15,L19- Note that NCCN was measured with a CCN counter in the other studies and the activated fraction was actually measured. So I would be careful in making very strong conclusions.

Response: The values of activated fraction for this study were found to be very high and N_{CCN} values were consistent with other polluted sites in the world based on size distribution data and chemical speciation data. It is the best that could be done with the data available at hand. However, I do believe that with the actual measurements, there can be new developments and any work of science is open to criticism based on scientific evidence, and so is this work.

Changes in the manuscript: None.

27. P31,Fig 1. In the uppermost subfigures the bars should be the mean values of NRPM. In the middle subfigs the sum of the constituents should be the same as in the upper subfigures. But they are not. What is wrong?

Response: Thank you for pointing this out. The figure has been corrected and is shown below.

Figure 3: Mean values of (a) $NRPM_1$ (b) Organics, inorganics and BC(c) PM1 species
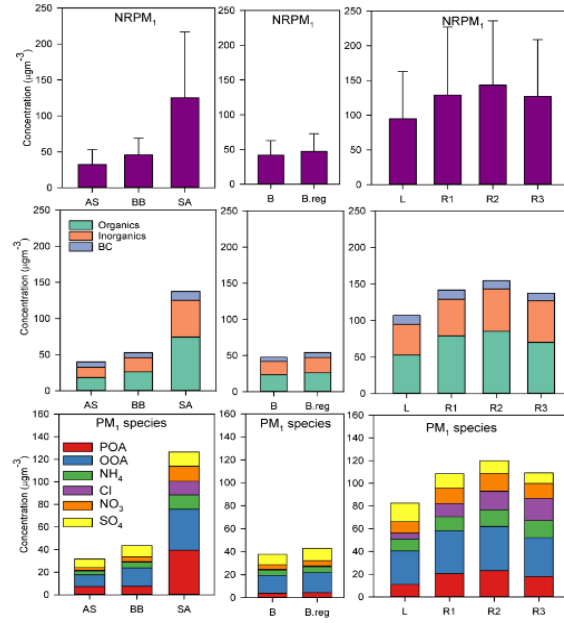
Changes in the manuscript: The corrections shown in Figure 3above have been included in Figure 2.

Air mass physio-chemical characteristics over New Delhi: Impacts on aerosol hygroscopicity and CCN formation

Zainab Arub[1], Sahil Bhandari[2], Shahzad Gani [3], Joshua S. Apte[3], Lea Hildebrandt Ruiz[2], Gazala Habib[1]

[1]Department of Civil Engineering, Indian Institute of Technology, Delhi, New Delhi, India

[2] McKetta Department of Chemical Engineering, The University of Texas at Austin, Texas, USA

[3]Department of Civil, Architectural and Environmental Engineering, The University of Texas at Austin, Texas, USA

Correspondence to: Zainab Arub (jyotika.mmmec@gmail.com)

Abstract.

Delhi is a megacity that is subjected to high local anthropogenic emissions and long-range transport of pollutants. This work presents for the first time time-resolved estimates of hygroscopicty parameter (κ) and CCN spanning for more than a year derived from chemical composition and size distribution data. This work presents for the first time long term and time-resolved estimates of hygroscopicty parameter (κ) and CCN for Delhi, a megacity that is subjected to high local anthropogenic emissions and long-range transport of pollutants. As a part of the Delhi Aerosol Supersite (DAS) campaign, characterization of aerosol composition and size distribution were conducted from January 2017- March 2018. Air masses originating from the Arabian Sea (AS), Bay of Bengal (BB) and South Asia (SA) exhibited distinct characteristics of time-resolved sub-micron non-refractory PM_1 ($NRPM_1$) species, size distributions, and CCN number concentrations. SA air mass had the highest $NRPM_1$ loading with high chloride and organics followed by BB air mass which was relatively more contaminated than AS with a higher organic fraction and nitrate. The primary sources were identified as biomass- burning, thermal power plant emissions, industrial and vehicular emissions. The average hygroscopicty parameter (κ), calculated by the mixing rule was ~ 0.3 (varying between 0.13 and 0.77) for all the air masses (0.32±0.06 for AS, 0.31±0.06 for BB and 0.32±0.10 for SA). The diurnal variations of κ were impacted by the chemical properties and thus source activities. The total, Aitken, and Accumulation mode number concentrations were higher for SA, followed by BB and AS. The mean values of estimated CCN number concentration (N_{CCN}, 3669-28926 cm^{-3}) and the activated fraction (a_f,

0.19-0.87) for supersaturations varying from 0.1-0.8% also showed the same trend (SA > BB > AS). The size turned out to be more important than chemical composition directly, and the N_{CCN} was governed by either the Aitken or Accumulation modes depending upon the supersaturation (SS) and critical diameter (D_c). The a_f was governed mainly by the Geometric Mean Diameter (GMD), and such a high a_f (0.71±0.14 for the most dominant sub-branch of SA air mass (R1) at 0.4% SS) has not been seen anywhere in the world for a continental site. The high a_f was a consequence of very low D_c (25-130 nm for SS ranging from 0.1%-0.8%) observed for Delhi. Indirectly, the chemical properties also impacted CCN and a_f by impacting the diurnal patterns of Aitken and accumulation modes, κ and D_c. The high hygroscopic nature of aerosols, high N_{CCN} and high a_f can severely impact the precipitation patterns of the Indian Monsoon in Delhi, the radiation budget and the indirect effect and need to be investigated to quantify the impacts.

1 Introduction

High aerosol loading can have huge climatic repercussions on precipitation including land surface feedback through rainfall, surface energy budget and variation in latent heat atmospheric influx (Tao et al., 2012). Added CCN may nucleate a larger number of smaller droplets, which then take a longer time to coalesce into raindrops (Gunn and Phillips, 1957; Squires, 1958). A greater cloud depth indicating higher rain initiation occurs in more polluted clouds. Complete suppression of warm rain might also occur and get aggravated due to additional CCN activation above the cloud base (Braga et al., 2017). While rain suppression has been observed in case of polluted urban and industrial plumes (Rosenfeld, 2000) and smoke arising from forest fires (Rosenfeld, 1999), the precipitation tendency increases due to influx of giant CCN consisting of sea salt (Rosenfeld et al. 2002) and salt playas (Yinon et al. 2002) due to acceleration of the auto-conversion rate (Rosenfeld et al. 2008). In order to understand the impact of pollution on indirect radiative forcing and precipitation in highly polluted regions, the information on CCN number concentration is essential in Global Climate Models (GCMs) and Regional Climate Models (RCMs).

As per the fifth IPCC report (Boucher et al., 2013), the two most important factors governing CCN activation and number concentration are size followed by composition. The aerosol chemical composition impacts the aerosol hygroscopicity which impacts the critical diameter and hence CCN activation. The hygroscopicity parameter (κ) has been defined as the total water uptake ability of aerosols (Petters and Kredenweis, 2007). Further, the increase in relative humidity (RH) due to water uptake by aerosol can impact visibility (Lee et al., 2016; Liu et al., 2012), secondary particle formation (Ervens et al., 2011) and measurements of remote sensing (Wang et al., 2007; Brock et al., 2016), aerosol loading and its chemical composition (Chen et al., 2018). Hence,

it is essential to determine the hygroscopicity of aerosols especially in the polluted regions of the world where these impacts are expected to be highly significant.

Although the recent precipitation data during 1950-2011 averaged over July and August for Delhi reveals a significant decreasing trend, there has been an increasing trend in the frequency of heavy rainfall events and a decrease in the frequency of wet and rainy days when it rains for a shorter time period (Guhathakurta et al., 2015). These occurrences are most likely signatures of aerosols impacting the cloud nucleating properties which calls for detailed CCN data examination. The high uncertainties associated with radiative forcings, both direct and indirect especially at the regional level are a result of poor representation of the aerosol distributions in GCMs. This is critical for the Indian sub-continent where the variability in aerosol microphysical properties is very high at various spatial and temporal scales. These necessitate the measurement of long term aerosol physiochemical properties, hygroscopicity parameter, and CCN estimates. Detailed CCN and κ measurements in India have been carried out in different parts of the world (Rissler et al., 2004; Bougiatioti et al., 2012; Engelhart et al., 2011)and in India at places like Kanpur (Bhattu et al., 2015; Bhattu et al., 2014; Ram et al., 2014), Mahabaleshwar (Leena et al.,. 2016), and eastern Himalayas (Roy et al., 2017). However, no CCN measurements or estimates have been developed so far for Delhi. There has been only one study that has estimated aerosol hygroscopicty based on $PM_{2.5}$ mass, RH and visibility data (Wang et al., 2019). In this work, for the first time for Delhi, time-resolved size distribution and chemical speciation measurements have been carried out from 15th January 2017- 31st March 2018 as a part of the DAS campaign (Gani et al., 2019). The time-resolved hygroscopicity parameter and CCN estimates have been derived using chemical speciation data from Aerosol Chemical Speciation Monitor (ACSM), and number concentration data from Scanning Mobility Particle Sizer (SMPS) measured during January 2017 to March 2018. Data has been analyzed to investigate the hypotheses: (a) the precursors to SOA formation critically impact the chemical composition over Delhi; (b) the emission sources significantly impact CCN formation by governing the size distributions and chemical composition, and thus hygroscopicity; (c) physical properties impact CCN more compared to chemical properties directly; however, the physical properties are in turn, shaped by the chemical properties.

2 Methodology and Instrumentation

2.1 Instrumentation

For a detailed assessment of aerosol physiochemical properties, Scanning Mobility Particle Sizer (SMPS, TSI, Shoreview, MN), Aerosol Chemical Speciation Monitor (ACSM, Aerodyne Research, Billerica MA) and Aethalometer (Magee Scientific Model AE33, Berkeley, CA) were operated at Indian Institute of Technology, Delhi in Block 5 at a height of nearly 15 m as a part of the Delhi Aerosol Supersite (DAS) campaign. This sampling

3

site at New Delhi was free from any source activity except for a road 150 m away. The IIT campus is relatively cleaner than the rest of the city. However, it lies in the heart of the city, and the outskirts of the campus experience fresh traffic influx. The IIT campus allows only limited access to vehicles and therefore has relatively lesser traffic compared to the city in general. A temperature controlled room was used to carry out the measurements. Two

5   separate and thermally insulated sampling lines (3/4 inch outer diameter stainless steel tubes) with flows of 3 LPM and 2 LPM equipped with PM_1 cyclone, in line with a water trap and a Nafion membrane diffusion dryer (Magee Scientific sample streamdryer, Berkeley, CA) were used for 1) SMPS and ACSM in conjunction with a flow controller 2) Aethalometer respectively. A brief description of the instruments is given below. A detailed description of the instruments can be found in Gani et al., 2018 and Bhandari et al., 2019.

10 The SMPS comprised of a differential mobility analyser analyzer (DMA, TSI 3081), an electrostatic classifier (TSI, 3080), X-ray aerosol neutralizer (TSI, 3088), and a water-based condensation particle counter (CPC, TSI 3785). The ambient air was sampled in the size range 12 nm- 560 nm, with a time difference of 135 s between two scans. The sheath to aerosol flow was 4:1 and the total flow drawn by the CPC being is 1 LPM. The two dominant modes (Aitken and Accumulation) are well captured within this size range. ACSM sampled the inlet air

15 at a flow rate of 0.1 LPM with a time resolution of ~1 min. The calibration procedures and data processing have been discussed in Gani et al., 2018. ACSM collected time-resolved $NRPM_1$ (Non-refractory Particulate Matter) based on species that volatilize by $600°$ C and included NO_3^-, Cl^-, SO_4^{2-}, NH_4^+, and organics.

2.2 Qualitative separation of organic aerosols as BBOA, HOA, and OOA

The composition data presented here were collected in the Delhi Aerosol Supersite (DAS) study. While the team
20 conducted PMF analysis on the 15 months in the dataset, they could resolve BBOA as a separate factor only in Spring 2018. They attributed this inability to resolve primary organic aerosol (POA) to separate factors hydrocarbon like organic aerosol (HOA) and biomass burning organic aerosol (BBOA) to the unit mass resolution of the instrument (Bhandari et al., 2019) and references therein). In lieu of the lack of explicit BBOA and HOA separation in all seasons, Ng et al., 2010 compilation of profiles was were analyzed combined with the profiles
25 identified in Spring in Delhi (since they separated POA to HOA and BBOA) in the DAS study. We observed that spring 2018 profiles fall within the bounds of the uncertainty of Ng et al. compilation. Thus, Ng et al. reference profiles were utilized for source attribution of each cluster. While factor profiles can differ across the world, taking regionally relevant profiles together with those usually employed as reference profiles for PMF analysis likely accounts for this variability. As a part of the analysis conducted here, we utilize both the mean strength at the
30 relevant m/z(s) (m/z 57 and 60) as well as the standard deviation (S.D.) of the profiles at these m/z(s) in the analysis.

Organic aerosols were qualitatively segregated by comparing the m/z ratios of f57 and f60 with the reference profiles of BBOA (f57: 0.0337±0.00884, f60: 0.025±0.00521), HOA (f57: 0.0838±0.00378, f60:

0.00227±0.00214) and OOA (f57: 0.00997±0.00786, f60: 0.00571±0.00349) as reported by Ng et al., 2010. This was done by first calculating the cluster means of f57 and f60 for each cluster (Table 2). This was followed by an evaluation of residuals. Residuals represent the deviation of the cluster means from the reference profiles. The HOA, BBOA and OOA residuals (R_{HOA}, R_{BBOA} and R_{OOA}) were then calculated based on cluster means of f57 and f60 (CM_{f57} and CM_{f60}) with respect to the corresponding means of reference profiles (RM_{f57} and RM_{f60}), as given below for HOA in Eq 1:

$$R_{HOA} = \sqrt{(CM_{f57\_HOA} - RM_{f57\_HOA})^2 + (CM_{f60\_HOA} - RM_{f60\_HOA})^2} \tag{1}$$

The reference residuals for HOA, BBOA, and OOA (R_{Ref_HOA}, R_{Ref_BBOA}, R_{Ref_OOA}) were then calculated using standard deviations of reference profiles ($SD_{f57\_Ref\_HOA}, SD_{f57\_Ref\_BBOA}, SD_{f57\_Ref\_OOA}$) as given below for HOA in Eq 2:

$$R_{Ref\_HOA} = \sqrt{(SD_{f57\_Ref\_HOA})^2 + (SD_{f60\_Ref\_HOA})^2} \tag{2}$$

The residuals of the cluster means were then compared with the reference residuals as per six conditions described in detail in Text S1 and classified as HOA, BBOA, OOA or mixed.

The following checks were then carried out for all clusters:(a) If $R_{HOA} < R_{Ref\_HOA}$, then aerosols are HOA, else if $R_{BBOA} < R_{Ref\_BBOA}$, then aerosols are BBOA else if $R_{OOA} < R_{Ref\_OOA}$, then aerosols are OOA else mixed, (b) If $R_{BBOA} < R_{Ref\_BBOA}$, then aerosols are BBOA, else if $R_{HOA} < R_{Ref\_HOA}$, then aerosols are HOA else if $R_{OOA} < R_{Ref\_OOA}$, then aerosols are OOA else mixed, (c) If $R_{OOA} < R_{Ref\_OOA}$, then aerosols are OOA, else if $R_{BBOA} < R_{Ref\_BBOA}$, then aerosols are BBOA else if $R_{HOA} < R_{Ref\_HOA}$, then aerosols are HOA else mixed, (d) If $R_{OOA} < R_{Ref\_OOA}$, then aerosols are OOA, else if $R_{HOA} < R_{Ref\_HOA}$, then aerosols are HOA else if $R_{BBOA} < R_{Ref\_BBOA}$, then aerosols are BBOA else mixed, (e) If $R_{HOA} < R_{Ref\_HOA}$, then aerosols are HOA, else if $R_{OOA} < R_{Ref\_OOA}$, then aerosols are OOA else if $R_{BBOA} < R_{Ref\_BBOA}$, then aerosols are BBOA else mixed and (f) If $R_{BBOA} < R_{Ref\_BBOA}$, then aerosols are BBOA, else if $R_{OOA} < R_{Ref\_OOA}$, then aerosols are OOA else if $R_{HOA} < R_{Ref\_HOA}$, then aerosols are HOA else mixed. If all 6 conditions were evaluated as the same specific category (i.e. HOA or BBOA or OOA), then that category was considered as the aerosol type for a cluster else they were considered as mixed.

2.3 Estimation of κ and CCN:

The ACSM data was used to calculate κ as per the following mixing rule in Eq. 3 (Petters and Kredenweis, 2007):

$$\kappa = \sum_i \epsilon_i \kappa_i \tag{3}$$

where, ϵ_i and κ_i represent the volume fractions and individual hygroscopicity parameters of the various components. The inorganics were represented by $(NH_4)_2SO_4$, NH_4Cl, and NH_4NO_3. The organic κ_i was taken as 0.1 (Gunthe et al., 2010; Gunthe et al., 2011; Dusek et al., 2010; Rose et al., 2011). and for all inorganic salts, κ_i values were taken from Petters and Kredenweis, 2007. κ_i values were taken as 0.61 for $(NH_4)_2SO_4$, 1.02 for NH_4Cl
5   and 0.67 for NH_4NO_3 (Sullivan et al., 2009; Petters and Kredenweis, 2007). The density values to estimate the volume fraction of the inorganic constituents were taken as 1770kg m^{-3} for $(NH_4)_2SO_4$, 1519 kg m^{-3} for NH_4Cl and 1720 kg m^{-3} for NH_4NO_3 (CRC Handbook of Physics and Chemistry, 95th Edition). The density of organics was taken as 1500 kg m^{-3} (Bougiatioti et al., 2009). κ for BC has been taken as zero in several studies in the past (Hong et al., 2014, Leng et al., 2014, Wu et al., 2013).

10   It should be noted that we assume that the κ calculated from NRPM$_1$ data of ACSM has been taken to represent the bulk hygroscopicity parameter in the absence of size-resolved measurements and is a limitation of this work. The difference due to the assumption cannot be accounted for and should be investigated in the future. However, it is reported that for $\kappa > 0.1$, CCN closures within 20% can be achieved assuming bulk composition and internal mixing (Wang et al., 2010). Temperature, relative humidity (RH), and the calculated κ were then used to calculate
15   the critical diameter (Dc) from the multi-component κ-Kohler theory (Bhattu et al., 2015). The temperature and RH data are available from the RK Puram site (~ 3-4 km aerial distance from the measurement site) maintained by the Central Pollution Control Board, India. N$_{CCN}$ was then estimated by integrating the size distribution obtained from SMPS above D$_c$. The CCN estimates were obtained for supersaturations (SS) = 0.1%, 0.15%, 0.2%, 0.35%, 0.4%, 0.5%, 0.6%, 0.7%, 0.75%, 0.8%, 0.85% and 1%. However, for the sake of detailed analysis, 0.1%,
20   0.4%, and 0.8% have been chosen. 0.1% represents the condition when the effect of chemical composition is expected to be the highest, 0.4% represents the condition for convective clouds and 0.8% represents a high supersaturation state when almost all aerosols would have a tendency to get activated as CCN.

2.4 Airmass characterization

In order to characterize the air masses, the Hybrid Single Particle Lagrangian Integrated Trajectory (HYSPLIT)
25   model was used (Draxler and Rolph, 2003) to determine the major pathways of aerosols reaching Delhi. The 5-day back trajectory analysis was done at the receptor site at a height of 500 m. The cluster analysis was then performed seasonally to identify the cluster mean trajectories per season. These mean trajectories were then again re-clustered to identify three main clusters based on the directions of the mean cluster trajectories as the Arabian Sea (AS) branch (16.5% of total trajectories), the Bay of Bengal (BB) branch (13% of total trajectories) and the
30   South-Asian (SA) branch (70.5% of total trajectories). The BB branch was further classified as B (54%) and B.reg (45%), where B represents the air masses reaching the sea, while B.reg represents the air masses aligned towards reaching the Bay of Bengal but did not hit the sea. The SA branch was partitioned into L (17.5%), R1 (54%), R2 (18%) and R3 (11%) where L represents the local trajectories originating within India, and mainly from Delhi,

Punjab and, Haryana, R1 represents trajectories coming from Pakistan and Afghanistan, R2 represents trajectories originating from Iran, and R3 is representative of all trajectories beyond including a portion of South Africa, Mediterranean Sea, and Turkey. The seasonal clusters for winter, spring, summer, and monsoon of the year 2017 and winter and spring of the year 2018 have been shown in Figure S1. The re-clustering has been shown in Figure 1. All the chemical speciation data from ACSM and size distribution data from SMPS were then categorized as per the classification discussed above and have been used in the following discussion.

2.5 Aerosol aging estimation

The NOx, toluene and benzene data inventory for the entire campaign was taken from CPCB for RK Puram, whenever available. The data was not available for branch B. To determine the photochemical aging of aerosols, toluene and benzene concentrations were used to calculate the life (in hours) as per Nault et al., 2018 in Eq (4):

$$t = -\frac{1}{[OH] \times (k_{toluene} - k_{benzene})} \times \left(ln\left(\frac{toluene_i\,(t)}{benzene_i(t)}\right) - ln\left(\frac{toluene_i\,(o)}{benzene_i(o)}\right) \right) \tag{4}$$

where, $[OH] = 1.5 \times 10^6$ molecules/cm^3 (Nault et al. 2018), $k_{toluene} = 2.3 \times 10^{-12}$exp (-190/T) and $k_{benzene} = 1.8 \times 10^{-12}$exp (340/T) (Atkinson et al., 2006) are the rate constants for each aromatic compound, $toluene_i\,(o) = 1.85$, $benzene_i\,(o) = 2.31$. The [OH] concentration is not constant and varies considerably temporally and spatially, but due to the unavailability of data pertaining to its variation for Delhi, it has been assumed constant for aging calculation.

3 Results and Discussion

The HYSPLIT analysis reveals that the north-west direction is the most dominant direction which is representative of SA air masses, and within it, R1 is the most dominant indicating that on an overall basis, the emissions from Pakistan and Afghanistan regions and the sources en route govern Delhi's aerosol characteristics. However, the chemical signatures are potentially different for the various clusters, which explains the variation of aerosol properties with time. Due to the different nature of sources and pathways, aerosol properties vary resulting in different hygroscopic properties and CCN forming potential. These aspects are discussed in the following sections.

3.1 Introduction to characteristics and sources of air masses

Out of the three main branches, the SA branch is the most anthropogenically contaminated followed by BB and AS branches as indicated by the mean NRPM$_1$ mass concentrations: 125.2±91.6, 45.9±23.3, and 32.5±20.6 μg m^{-3} respectively (Figure 2a). The total NRPM$_1$ loading for the SA branch follows the sequence: L < R3 < R1< R2.

Amongst the SA branches, L is associated with the lowest organic (52.8±40.6 µg m⁻³) and inorganic (42.1±33.1 µg m⁻³) content while R2 has the maximum organic (85.4±59.8 µg m⁻³) and inorganic (57.9±47.5 µg m⁻³) content. A summary of the overall characteristics has been given in Table 1. L air-masses travel mainly over the Delhi-National Capital Region (NCR) region, Punjab and Haryana while R1 refers to air-masses originating from Pakistan and Afghanistan. The prominent sources for SA air mass include metal processing industries (Haryana and Delhi NCR), coke and petroleum refining (Punjab), thermal power plants (Pakistan, Punjab and NCR Delhi), agricultural residue burning (Punjab and Haryana), soil dust (Pakistan, Punjab) (Jaiprakash et al., 2017) and coal mines in Pakistan where non-ideal burning of $(NH_4)_2SO_4$ occurs (Chakraborty et al., 2015).

On comparing the BB branches, total $NRPM_1$ for B (41.9±20.8 µg m⁻³) is slightly lesser than ~~that for~~ B.reg (47.3~~50.7~~±25.4 µg m⁻³) and can be attributed to the fact that B.reg air mass does not travel over water (originates adjacent to ~~the~~ coastline) but nevertheless is subject to its influence while B air mass travels over water and is therefore relatively cleaner. B.reg has ~~a slightly higher i~~lesser inorganic and more organic content than ~~that of~~ B.

The relatively higher abundance of aerosols of BB over AS can be attributed to both the sources and the pathways of air masses. In terms of source, the Bay of Bengal is more anthropogenically impacted than the Arabian Sea as concluded by the ICARB campaign (Kalapureddy et al., 2009). Previous studies (Nair et al., 2008a, 2008b; Moorthy et al., 2008) reported higher aerosol number concentration (N_{CN}), as well as Black Carbon (BC) concentration over the Bay of Bengal than that of Arabian Sea in all size ranges within the marine boundary layer as well as the vertical column. The BB air mass travels over the Indo-Gangetic Plains and the AS air-mass travels across Western India and the desert region of Rajasthan. Based on previous emission estimates (Habib et al., 2006) the emission fluxes from fossil fuel dominate the aerosol burden over the Indo-Gangetic plains (IGP). The aerosol over IGP is largely composed of Inorganic oxidized matter (IOM) including fly ash from coal-fired power plants and mineral matter from open crop waste burning (Habib et al., 2006). The AS air mass travels over western India and brings pollution from both fossil fuel combustion and desert dust (Habib et al., 2006).

3.2 PM₁ chemical composition of different air masses

Mass closure between SMPS size distribution data and the sum of ACSM species together with BC was achieved (R^2= 0.83) as detailed in our parallel manuscript Gani et al. 2019. The $NRPM_1$ species (NH_4^+, Cl^-, NO_3^-, SO_4^{2-}, POA, and OOA) and BC vary significantly for the different air-masses both in terms of the mass of species (Figure 2c) and the diurnal patterns (Figure 3), leading to different aerosol chemistry and chemical reactions. A summary of the average mass of each species for all air masses is detailed in Table 1. In brief, both POA and OOA followed

by NO_3^-, SO_4^{2-} and Cl^- dominated the PM composition for the SA air mass, while OOA followed by SO_4^{2-} and OOA was dominant for BB and AS air masses. High chloride is a special feature of the SA air mass, which is not apparent in the other two branches.

NH_4^+ has been assumed to be the dominant cation based on high Aerosol Neutralization Ratio (ANR) values (mean values ranging from 0.95-0.85). calculated as per Zhang et al., 2007 ANR is defined as the normalized ratio of the measured NH_4^+ concentration to the NH_4^+ concentration needed for full neutralization of the anions and calculated as per Eq. (5) (Zhang et al. 2007).

$$ANR= \frac{NH_4^+\,meas}{NH_4^+\,neut} = \frac{(NH_4^+/18)}{(2 X SO_4^{2-}/96)+(NO_3^-/62)+(Cl^-/35.5)} \tag{5}$$

. Detailed ANR values have been given in Table S1. ANR values reveal that while AS, B, and L branches were completely neutralized, B.reg, R1, R2, and R3 were only partly neutralized indicating that minor components of sulphate, chloride, and nitrate may be bound to non-volatile salts such as $NaNO_3$ or $NaCl$ or Na_2SO_4 or are associated with organics as organosulphates, organochlorides, or organonitrates, evidence for which has been shown in a previous DAS study (Bhandari et al., 2019).

To determine the dominant salts, NH_4^+ ions were neutralized with SO_4^{2-} ions. The speciation of salts of NH_4^+ and SO_4^{2-} was determined by the molar ratio of NH_4^+ to SO_4^{2-} ions ($R[SO_4^{2-}]$). $R[SO_4^{2-}] > 2$ is indicative of $(NH_4)_2SO_4$, while $1 < R[SO_4^{2-}] <> 2$ indicates a mixture of $(NH_4)_2SO_4$ and NH_4HSO_4 and $R[SO_4^{2-}] < 1$ indicates a mixture of H_2SO_4 and NH_4HSO_4 (Nenes et al., 1998; Asa-Awuku et al., 2011; Padro et al., 2012). For Delhi, $R[SO_4^{2-}] > 2$ was obtained for all branches indicating that $(NH_4)_2SO_4$ is present in all branches. Furthermore, the non-sulphate NH_4^+ ions $[ns\text{-}NH_4^+] = [NH_4^+] - 2 \times [SO_4^{2-}]$ were then checked for coupling with Cl^-, NO_3^- and $[NO_3^- + Cl^-]$ ions jointly with r^2 values as a criterion (Du et al., 2010). All r^2 values have been detailed in Table S1. This analysis revealed that $(NH_4)_2SO_4$ is the dominant salt for AS and B branches based on $r^2_{NH4+/SO42-}$ values of (0.78 for AS, and 0.75 for BB 0.75. NH_4Cl formation for SA was confirmed by high r^2 value (0.90) for $ns\text{-}NH_4^+$ coupling with Cl^-. A similar finding has been reported by Bhandari et al., 2019 based on the coupling of the NH_4Cl factor with wind direction. Coupling of $ns\text{-}NH_4^+$ with NO_3^- revealed a good correlation for B (0.70) and B.reg (0.63) (Figure S6).Coupling of $ns\text{-}NH_4^+$ with NO_3^- revealed a good correlation (0.70) for B. In all cases, an increase in r^2 for combined $NO_3^- + Cl^-$ as compared to individual ions indicated that both HNO_3 and HCl are synchronously neutralized by NH_3. If Cl^- and NO_3^- are present in fine mode, they are expected to be in the form of their respective ammonium salts (Harrison and Pio, 1983). Thus, the dominating salts are $(NH_4)_2SO_4$ for AS, $(NH_4)_2SO_4$ and

NH$_4$NO$_3$ for BB air-mass and NH$_4$Cl for SA and its sub-branches.Thus, the dominating salts are (NH$_4$)$_2$SO$_4$ for AS and B.reg, (NH$_4$)$_2$SO$_4$ and NH$_4$NO$_3$ for B branches and NH$_4$Cl for SA and its sub-branches.

The organic speciation revealed that AS organics were as associated with BBOA, BB organics wherein both B organics and B.reg organics were associated with all 3 mixed organics and SA organics were was associated with

5   BBOA wherein L, R11, and R2 organics were associated with BBOA and   R3 organicswas included associated with both HOA and BBOA.

The NOx emissions (in μg m^{-3}) for SA air mass (96.88±127.22) weare the highest followed by that in BB (38.30±64.79) and then in AS (36.71±68.13) air mass. BB is actually representative of B.reg only as NOx data for B air mass was not available and AS values were also scarce. The SA aerosols exhibited less aging (4.38±4.49

10   h) compared to B.reg. (11.58± 3.45 h), but both were representative of aged aerosols. Aging was not calculated for AS due to very little data availability.

In order to determine the presence of biomass burning and traffic emissions, BCwb (wood-burning component) and BCff (traffic component) for all air masses were determined based on Aethalometer data as per Sandradewi et al., 2008. The contribution of BCwb and BCff have been summarized in Table S4. Since fossil fuel sources

15   are active the year-round, there is a strong presence of BCff ranging from 70% to 86%. However, biomass burning is only active during certain specific times for short durations and is very prominent in the north-west direction for the SA air masses. It was observed that the more distant air masses exhibited a higher BCwb contribution compared to those originating within close proximity. Hence, while L was associated with 13.9% BCwb, R3 exhibited 29.2%BCwb. The BCwb contribution for A and BB air masses was 21%. It can thus be concluded that

20   both biomass burning and traffic emissions are important sources contributing to the chemical composition of the various air masses.

3.3 Diurnal variation of chemical species and probable sources

The South-Asian air mass: This air mass ranks highest in NH$_4^+$ ion concentrations compared to other branches. Locally (i.e. for L), the source for NH$_4^+$ may be attributed to NH$_3$ gas from the nearby agricultural fields of the

25   Indian Agricultural Research Institute (IARI) (Sharma et al., 2014). For R1, R2, R3, sharp spikes in early morning hours seen in the diurnal patterns of NH$_4^+$ indicate its formation from ammonia as a result of industrial exhausts of untreated ammonia. This is because its diurnal variation is very similar to the diurnal of NH$_3$ emissions of industrial origin (Wang et al., 2015). A very prominent feature of the SA that makes it distinct from the other two

air-masses is the presence of high chloride (L < R1 < R2 and R3). High Cl^- in the SA branch can be attributed to several factors: (a) Khewra salt mines in Pakistan might contribute to high Cl^- in other branches compared to L; (b) Locally, plastic burning, refuse burning and soil dispersion; (c) Biomass Burning, which is a very prominent feature of the SA branch as indicated by f57 and f60 values, and is also indicated by thea large number of fire counts from MODIS fire-count data (Bhattu et al., 2015), dominantly in Punjab and Haryana and few places in Pakistan; (e) Coal-based thermal power plants in Delhi, Punjab, Haryana and Pakistan; (f) Small and medium scale metal processing industries in Delhi, Punjab, and Haryana where HCl is used in pickling process of hot and cold rolling of steel sheets and acid recovery from fume generation is not practiced (Jaiprakash et al., 2017).

As far as the increase in chloride with the increasing length of trajectories is concerned, the most plausible explanation is biomass burning. It has been pointed out in Section 3.2 earlier that BCwb contribution increases as the air mass trajectories become distant, a feature similar to chloride emissions. There is a marked similarity in the diurnal patterns of NH_4^+ and Cl^- ions such that L < R1< R2 < R3 is true for both $[Cl^-]$ and $[NH_4^+]$ indicating the formation of NH_4Cl. NH_4Cl may also be emitted directly from cement plants (Cheney et al., 1983) in Punjab. The equilibrium constant for Cl^- is more sensitive to ambient temperature than NO_3^- as a result of which during daytime a large amount of NH_4Cl dissociates to form NH_3 and HCl if the temperature exceeds $10^{\circ}C$ (Kaneyasu et al., 1998). The diurnal patterns of both $[NH_4^+]$ and $[Cl^-]$ exhibited a sharp decrease after 08:00 in the morning which is obvious since NH_4^+ for SA air mass is mostly associated with Cl^-. At the same time $[NO_3^-]$ showed an increase between 9:00-10:00 and then started decreasing, but the rate of decrease was relatively lower than NH_4Cl. This is expected as NH_4NO_3 is relatively more stable than NH_4Cl (Kaneyasu et al., 1998). During winter the ambient temperature drops slightly below $10^{\circ}C$ in the morning hours and then increases sharply after 08:00 to reach a maximum at 14:00, then again starts decreasing and reaches around $10^{\circ}C$ at mid-night (Gani et al., 2019). Since during winters, the air mass comes majorly from the north-west direction of SA air mass, it is evident that the formation and dissociation of NH_4Cl were governed by the ambient temperature at the receptor site.

The reduction in chloride concentrations chloride depletion during mid-day can also be attributed to sulphate substitution mechanism when sulphate formation enhances and is also marked by the ratio $R[SO_4^{2-}]$ ratio being greater than two for L, R1, R2, and R3. This is valid especially for L where $[SO_4^{2-}]$ increases significantly. However, the diurnal patterns of $[SO_4^{2-}]$ and $[NH_4^+]$ did not resemble each other, indicating that $(NH_4)_2SO_4$ may be present in small amounts but primarily SO_4^{2-} is associated elsewhere. Hence, SO_4^{2-} in combined form can be expressed in two ways: (a) small amounts of $(NH_4)_2SO_4$ (b) majorly in combination with K^+. Thus, the sharp jump in $[SO_4^{2-}]$ in locally originated air masses in the late morning and afternoon hours may be attributed to SO_2

11

emissions. SO_2 emissions in India are primarily attributed to power generation plants that make use of coal combustion as the chief source (Reddy and Venkataraman, 2002) followed by transportation. Such coal-based power plants are located in the IGP, with a high concentration in Haryana. SO_2 dissolves readily in water and can form sulphite ion, which in the presence of ozone can form sulphate ion (Erickson et al., 1976). H_2SO_4 formed from the reaction of SO_2 and ozone can react with NH_3 to form NH_4HSO_4, which combines with NH_3 again to form $(NH_4)_2SO_4$ (Stelson et al., 1982; Seinfeld 1986). Since the ozone spikes in the morning from10:00-16:00, more sulphate formation is seen when ozone is maximum. The diurnal variation for ozone has been explained in Gaur et al., 2014 for Kanpur where a spike in ozone levels is seen from 10:00- 16:00. A peakHike in sulphate concentration has also been previously observed for the foggy period in Kanpur at 10:00 due to the resumption of photochemical activity after fog dissipation (Chakraborty et al., 2015). SO_4^{2-} in SA branches may also combine with K^+ as K^+ is produced in biomass burning. It has already been mentioned that biomass burning is a highly significant feature of SA branches. Evidence for the presence of K^+ along with SO_4^{2-} in accumulation mode has been reported in Fuzzi et al., 2007. SO_4^{2-} and NO_3^- emissions may also be associated with secondary formation for R1, R2, and R3 due to industrial emissions from metal product manufacturing industries in Punjab and Haryana, large-scale manufacturing of porcelain insulators, switchgear in Islamabad (Jaiprakash et al., 2017) and steel rolling mills in Iran, Iraq, and Turkey and Punjab.

The NO_3^- levels are very high for SA. The high NO_3^- in SA can be explained due to the non-ideal burning of NH_4NO_3 and NOx emissions due to mining equipment in the coal mines in Pakistan leading to high NO_3^- formation (Chakraborty et al., 2015). It has been mentioned in Section 3.2 that NOx emissions in the SA branch are very high. NH_4^+ neutralizes NO_3^- simultaneously with Cl^-, however, the correlation of $[NO_3^-]$ with $[ns-NH_4^+]$ is moderate for SA. Therefore, it is expected that NO_3^- might be associated with K^+ and Na^+ since biomass burning results in K^+ and Na^+ emissions (Fuzzi et al., 2007). It has been shown that K^+ and Na^+ exhibit a high affinity for nitrate during neutralization reactions, thus aiding in particulate nitrate formation (Bi et al., 2011). This is in addition to other nitrate sources that have been discussed above along with SO_4^{2-} sources for SA.

The BC concentrations are highest for SA followed by that in AS and then in BB. The biomass burning in SA air mass could be a major source of BC besides power plants, cement plants, local traffic, and industries. The POA emissions for SA followed the order L < R3 < R1< R2. The spikes during early morning hours and night time of the POA diurnal profile may be attributed to lower boundary layer heights during the two periods. BC and POA are well correlated ($r^2 = 0.77$) for R3, indicating that they are coming from primary emissions. The diurnal profiles for all branches are similar which shows a decline as the day proceeds followed by an increase as the night

12

proceeds. OOA is present significantly in all the three branches, but is maximum for SA. Its diurnal variation resembles that of NO_3^- ($r^2 = 0.78$) indicative of its semi-volatile nature. OOA and NO_3^- correlations are strongest for L ($r^2 = 0.91$), followed by R2 ($r^2 = 0.85$), R3 ($r^2 = 0.81$), and R1 ($r^2 = 0.75$).

The Bay of Bengal air mass: [Cl$^-$] was lower in this air mass compared to SA. For both of the BB branches, fossil fuel combustion is the most likely source of Cl$^-$ as fossil fuel emissions dominate IGP. Cl$^-$ for BB is not correlated with ns-NH_4^+ and may probably be present in the form of methyl chloride, methylene chloride, carbon tetrachloride and tetrachloroethene (Ho et al., 2004).

Fossil fuel combustion from coal plants along IGP can be explained as a common source for both SO_4^{2-} and NH_4^+ ions, leading to $(NH_4)_2SO_4$ formation ($r^2_{NH4+/SO42-} = 0.78$). This is also seen in the diurnal profiles of both [SO_4^{2-}] and [NH_4^+] both of which exhibit a sharp spike in the early morning hours between 10:00-16:00. SO_2 emissions as explained for SA via photochemical oxidation by O_3 in combination with NH_3 can lead to $(NH_4)_2SO_4$ formation. For B.reg branch, the diurnal profiles of NH_4^+ and SO_4^{2-} exhibit double spikes (M-pattern, which is a typical feature of NOx profile for traffic emissions) during heavy traffic hours (06:00-08:00 and around 16:00-19:00), indicating $(NH_4)_2SO_4$ formation. NO from automobile exhausts can also form NH_3 in three ways catalytic convertors (Gandhi and Shelf, 1991) which in combination with SO_2 formed due to pyrolysis of sulphide fuels and subsequent oxidation, can lead to $(NH_4)_2SO_4$ formation.

The correlation of [NO_3^-] with [ns-NH_4^+] was found to be appreciably high for both B and B.reg. For both of these branches, the fossil fuel combustion resulting in NO_3^- emissions in combination with NH_4^+ (Rajput et al., 2015; Pan et al., 2019) can lead to NH_4NO_3 formation. The correlation of [NO_3^-] with [ns-NH_4^+] was found to be very poor for B.reg and was appreciably high for B. The NO_3^- present in B.reg might be associated with K$^+$, Na$^+$, and Ca^{2+} in the accumulation mode. NO_3^- has been found to be associated with the same in light-duty vehicles with oil additives as a possible source (Sodeman et al., 2005). For B, fossil fuel combustion resulting in NO_3^- emissions in combination with NH_4^+ (Rajput et al., 2015; Pan et al., 2019) can lead to NH_4NO_3 formation. This is also evident from the diurnal profile of NO_3^- that shows a very similar pattern to NH_4^+ and is expected to be in the form of NH_4NO_3. The diurnal profiles of NO_3^- show a decline as the temperature increases during the day and NO_3^- converts back to HNO_3, due to its semi-volatile nature.

The BC concentration in BB air masses was considerably lower than in the SA air masses. The missing points in the diurnal variability of BC for B region are on account of the unavailability of Aethalometer data. The BC in IGP can be emitted from industries (as for B), traffic (as for B.reg) and natural sources (Derwent et al., 2001). For

B and B.reg, the B.reg branch was subjected to a longer duration of anthropogenic influence compared to B which also spent a considerable time on the water, hence after the early morning hours, when the various fresh emissions start increasing, the magnitude of POA for B.reg exceeds B. However, POA for BB was quite low compared to SA. For B.reg, the spike in OOA during daytime hours is very similar to that of odd oxygen (O_3+NO_2) for Delhi, where the O_X profile for Delhi has been given in Tiwari et al., 2015, indicating its production by local photochemistry despite the increase in boundary layer height in the afternoon.

The Arabian Sea air mass: Chloride amounts are relatively very low for AS compared to SA. Biomass burning as indicated by f57 and f60 measurements seems to be the main Cl^- contributor to AS and might be associated with K^+ which is also emitted along with it.

Similar to L in the case of SA and BB, the power stations in Gujarat and Rajasthan lead to SO_2 emissions. Since the number of power plants is relatively lesser, the concentration is much lower compared to SA and BB air masses. SO_2 emissions subsequently lead to $(NH_4)_2SO_4$ formation which is the main salt present in this branch and is also evident from the high correlation between the two ions. $(NH_4)_2SO_4$ may be formed both due to emissions from power plants and traffic (similar to B.reg). Traffic emissions can be understood from the M-pattern in diurnal profiles of NH_4^+ and SO_4^{2-}, though the variation is not very pronounced, and might be suppressed due to power plant emissions. The traffic signal is more clearly implied by the diurnal profile of $(NH_4)_2SO_4$ for AS as seen in Figure S2. The correlation of $[NO_3^-]$ with $[ns-NH_4^+]$ was found to be very poor for AS indicating that NO_3^- might be associated with K^+ and Na^+ similar to B.reg.

Both BC and POA are quite less compared to SA.Both BC and POA for AS air mass are less than in the SA air mass. However, compared to BB, BC is slightly higher and POA is comparable. BC is likely to be of industrial origin. The POA diurnal profile is similar to the other air masses. Similar to B.reg, the OOA diurnal pattern resembles that of odd oxygen, where the odd oxygen profile has been reported in Tiwari et al., 2015.

Thus, it can be concluded that the direct emission sources and the pre-cursors (SO_X, NO_X, NH_3, O_3, and Ox) that lead to particulate matter formation, strongly impact the chemical properties of aerosols. The high PM1 concentration for Delhi which exceeds the National Ambient Air Quality Standards can be mitigated only by controlling both the primary emissions and precursors. In order to address the situation justly, following measures are lacking: a) Data enlisting measurements of PM_1 emissions from various industries in India and Asia, b) Description of the chemical constituents of aerosol that are being emitted, both qualitatively and quantitatively,

c) Defining emission limits and complying with the same. The chemical properties of aerosol also impact the hygroscopicty of aerosols as will be discussed in the following section.

3.4 Impact of chemical composition on the hygroscopicity of air masses

This study provides the first long term estimation of measurements of aerosol hygroscopicity in the PM_1 regime. The mean κ was the same for all the air masses which is ~ 0.3 (0.32±0.06 for AS, 0.31±0.06 for BB, and 0.32±0.10 for SA), as has been found to be the case for the global average of 0.27± 0.21 for continental aerosols. (Andreae and Rosenfeld, 2008; Petters and Kreidenweis, 2007; Pöschl et al., 2009; Pringle et al., 2010). Including BC in κ calculations leads to a difference of 10% in κ on an average, shifting the mean κ of 0.32 to 0.29. The BC mass fraction and volume fractions were 10% and 9% respectively. Thus, the change in κ due to the introduction of BC was not significant.

However κ varieds from 0.13-0.77, and there wais a difference in the diurnal variation of the hygroscopicity parameter for the various air masses (Figure 4). A similar finding was observed in China with a mean κ of 0.3 and varying in the range 0.1-0.5 (Rose et al., 2010). Recently, κ of 0.42±0.07has also been reported for $PM_{2.5}$ for Delhi based on Beta Attenuation Monitor (BAM) measurements of $PM_{2.5}$ (Wang et al., 2019), using an indirect method in the absence of direct measurements. Thus, the dependence of κ on size cannot be underestimated for Delhi and should be dealt with in the future. This points out to the fact that organic fraction is higher in the smaller size range while the inorganic fraction increases substantially with size. Similarly, an increase in mass growth factors at 97% RH has also been observed at the Slovenian coast and was measured as 6.95 for the smaller size range (0.53-1.6 μm) and 9.78 for the larger size range (1.6-5.1 μm) (Tursic et al., 2005). Aitken mode κ has been found to be 0.25 while accumulation mode κ was 0.45 for Beijing (Gunthe et al., 2011). Even in the PM_1 size range, while κ of 0.1 indicates secondary organic aerosol, κ has been found to vary from 0.01- 0.8 for biomass burning aerosols in lab studies (Peters et al., 2009). κ has also been found to vary from 0.15 to 0.25 with lower values (around 0.16) being observed during the night when biomass burning particles prevailed during wintertime at Athens, Greece (Psichoudaki et al., 2018)., Thus, indicating that κ values for Delhi can represent both secondary formation and biomass burning. This is true for Delhi which has both POA and OOA in all the air masses, while BBOA is present in AS and SA air masses as detailed in the preceding sections on chemical properties.

An important observation for all branches is that when the inorganic volume fraction (of dominant salt) increases (Figure S2) or during the times when κ is high (Figure 4) or when the organic volume fraction decreases (Figure S2), a dip in D_C (Figure 6) is seen, implying that a larger size regime is available for activation. The diurnal

variation of κ (Figure 4) follows more strongly the diurnal pattern of the dominant inorganic salts for a cluster as is evident from Figure S2 since the hygroscopicity parameters for inorganic salts are considerably higher than that of organics. Pearson correlation coefficient (r) values between κ and the salt volume fractions reveal that the diurnal patterns of κ were governed dominantly by volume fractions of $(NH_4)_2SO_4$ (r: 0.85) for AS, moderately

5   by $(NH_4)_2SO_4$ (r: 0.55) and NH_4NO_3 (r: 0.49) for BB and dominantly by NH_4Cl for SA air masses. For the two BB branches, κ of B branch was governed dominantly by $(NH_4)_2SO_4$ (r: 0.78) and moderately by $(NH_4)_2SO_4$ (r: 0.57) and NH_4NO_3 (r: 0.54) for B.reg. For SA air masses, κ of R1, R2, and R3 was governed dominantly by NH_4Cl (r values of 0.71, 0.89, 0.95) and jointly by NH_4Cl (r: 0.65) and NH_4NO_3 (r: 0.73) for L.

High volume fractions of $(NH_4)_2SO_4$ and NH_4NO_3 may be attributed to SO_x, NO_x, and NH_3 emissions due to power

10   plant emissions and traffic. In the SA sub-branches (Figure 4), the spike in κ during the early morning (07:00-08:00) exhibits the sequence: R3 > R2 > R1 >= L and the lower spike in late evening (18:00-22:00) exhibits R3 < R2 <R1 < L, and is attributed to NH_4Cl formation. This implies that during morning R3 aerosols are most hygroscopic while L aerosols are least hygroscopic, while after 09:00, L aerosols are most hygroscopic and R3 aerosols are the least hygroscopic. The flatter curve of κ can be attributed to two factors: (a) the chloride

15   contribution of distant trajectories decreases very steeply with time compared to the local emissions, and (b) κ of L is also supplemented substantially by NH_4NO_3. Thus, the source activities due to which the chemical properties of aerosols are shaped impact the hygroscopicity parameter tremendously. This consequently impacts the size regime of aerosols available for activation and has been discussed in the following section.

3.5 Impact of governing parameters on CCN estimates of air masses

20   CCN number concentration (N_{CCN}) for SA (22526±13439) is higher compared to BB (12526±5626) and AS (11089±6650), where values (cm^{-3})are given at 0.4% SS. Amongst the SA sub-branches, N_{CCN} followed increasing order as L (18810±9434) < R3 (20469±10580) < R2 (23736±13739) < R1 (24053±14743) while for the B branches, the order of increase in N_{CCN} (cm^{-3}) was B (11699± 4900) < B.reg (14088±6506), at 0.4% SS. Correspondingly, the activated fractions (a_f) follow the sequence: SA (0.70±0.15) < BB (0.64±0.17) < AS

25   (0.55±0.18) wherein for SA sub-branches, R3 (0.65±0.16) < R2 (0.694±0.16 < L (0.692±0.13) < R1 (0.71±0.15) and for BB, B.reg (0.62±0.16) < B (0.65±0.18), at 0.4% SS. Mean N_{CCN} and a_f for all branches at 0.1%, 0.4% and 0.8% SS have been detailed in Tables 3 and 4 respectively. The total number concentrations (N_{CN} in cm^{-3}) follow the sequence AS (20558±9654) < BB (20864±9731) < SA (31406±15168) and for SA, L (27009±11651) < R3

(30974±12223) < R1 (32772±16475) < R2 (33371±14989) and B (19025±7704) < B.reg (24333±11956). Mean N_{CN} for all branches has been listed in Table S2.

High values of N_{CCN} for Delhi are consistent with other polluted regions in the world. The relevant statistics for two highly polluted sites namely, Beijing and Kanpur are presented from Gunthe et al., 2011 and Bhattu et al., 2015 respectively. N_{CCN} has been found to be 7660± 3460 and 900-27000 (in cm^{-3}) at 0.46% SS and in the range 0.18-0.6% SS respectively. The high N_{CCN} is consistent with the high N_{CN}. Correspondingly, N_{CN} has been found to be 16800±9100 and ~50000 (cm^{-3}). Even though high number concentrations of CCN and CN have been reported, the a_f has not been found to be so high. The a_f in Beijing has been found to be 0.54±0.23and 0.66±0.23 at 0.46% SS and 0.86% SS respectively. For Kanpur, a_f has been reported to be ~0.018-0.54 for 0.18-0.60% SS. However for Delhi, the a_f ranges from 0.19 for AS at 0.1% SS to 0.86 for R1at 0.8% SS, implying that even at low SS, a considerably large number of particles are activated and at high SS, almost all particles reach the activated state. It should be noted here that the statistics for Beijing and Kanpur correspond to the range (3-900 nm) and (14.6-680 nm) while the estimates for Delhi have been given in the (10-560 nm) range. This finding is also consistent with Wang et al., 2019 which states that for Delhi, activation of a 0.1 μm particle requires SS ~0.18± 0.015% compared to ~0.3% for Beijing, 0.28–0.31% for Asia, Africa, and South America and ~0.22% for Europe and North America. The high activated fractions of aerosol can impact the precipitation patterns in Delhi and may be responsible for the short, intense precipitation events and decrease in overall rainfall. However, no study to date has validated this growing trend with CCN measurements or estimates and this needs to be investigated in the future.

The a_f and N_{CCN} for all air masses as expected increases with an increase in supersaturation. The variation of CCN and activated fraction with SS has been shown in Figures 5and S3. The figures clearly show that even though N_{CCN} for SA is far greater compared to BB and AS, the activated fractions are fairly close. B.reg has higher CCN but close a_f compared to B. Similarly, L has the lowest N_{CCN} among all SA branches but highest a_f. These features clearly elucidate that many factors are at play and impact N_{CCN} and a_f differently. In order to determine the governing parameters impacting both N_{CCN} and a_f, the diurnal patterns of N_{CCN}, a_f, D_c at 0.1%, 0.4% and 0.8% SS, N_{CN}, N_{Aitken}, $N_{Accumulation}$, κ, and GMD have been shown in Figures 6, S4 and S5.

The N_{CCN} curve for SA shows a sharp diurnal feature which is not as prominent for the other two. However, in the noontime at 0.4% and 0.8% SS, while CCN dips for SA, it rises for AS and BB (Figure 6). Further, with the increase in supersaturation, the dip in CCN of SA increases such that (a) at 0.1% SS, $SA_{CCN} > AS_{CCN}$, BB_{CCN}, (b)

at 0.4% SS, $SA_{CCN} \sim= AS_{CCN}$, $BB_{CCN,}$ and (c) at 0.8% SS, $SA_{CCN} < BB_{CCN}$ and $\sim= AS_{CCN}$. The explanation for this observation is that at 0.1% SS, the CCN is being governed by the accumulation mode but at 0.4% and 0.8% SS, it is being governed more by the Aitken mode. It is the Aitken mode that dominantly governs the total number concentration, and hence it can be said that CCN is being governed by CN at higher SS, and by the accumulation mode at low SS. This is because as supersaturation increases, D_c increases. At low SS, Dc is high ($D_c > 100$ nm) almost always at 0.1% SS for all branches as shown in Figure 6d, hence the size distribution that is being integrated to get the CCN involves the accumulation mode only. At 0.4% SS, the Dc was around 40-47 nm, therefore a considerable fraction of Aitken mode and accumulation mode is available for activation while at 0.8% SS the Dc was ~25-30 nm, therefore, the contribution of Aitken mode further increases and accumulation mode is also available as usual. These findings are also true for BB branches (B and B.reg) and SA branches (L, R1, R2, and R3) as shown in Figure S4. It is the low value of D_C relative to other places that is responsible for high CCN. As explained in Section 3.4, Dc is largely associated with κ. The D_C at other places such as Kanpur has been found to vary from 50-200nm for SS ranging from 0.18-0.60 (Bhattu et al., 2015), compared to which Dc for Delhi is lower (17-142 nm for SS ranging from 0.1%-0.8%), implying a larger regime is being available for activation. It would also be pertinent to mention here that the dip in CCN for SA during mid-day and the peakhike during the same for AS and BB can be attributed to the following. (a) The dip in $N_{Accumulation}$ for SA during mid-day is much more prominent compared to AS and BB. (b) During mid-day, the N_{Aitken} for SA also decreases while it increases for AS and BB. Thus, the dip in N_{CCN} is strengthened by the simultaneous dip of both Aitken and Accumulation modes while the peakhike in N_{CCN} for AS and BB is a manifestation of the dominant peakhike in Aitken modes. Similar features are also exhibited for sub-branches of BB and SA. A deeper insight reveals that the dip in number concentration during mid-day for SA is most aptly seen in the diurnal pattern of POA (which is the most dominant $NRPM_1$ species) and to quite a good extent in other $NRPM_1$ species barring SO_4^{2-} ion. Similarly, the peakhike in Aitken mode for AS and BB can be attributed to NH_4^+, SO_4^{2-} and OOA concentrations (the dominating species in the respective branches). Thus, the source activities and trajectory pathways impact CCN concentration at the receptor site.

The diurnal pattern for a_f shows a dip in the mid-day hours for all the air-masses even though N_{CCN} during mid-day for AS and BB peakhikes during mid-day hours. The time of dip in a_f (more prominent at 0.4% and 0.8% SS) occurs earlier for AS compared to BB and SA (Figure 6). This is governed by the time of dip in the Geometric Mean Diameter (GMD) of the three branches. The GMD diurnal variation is very similar to a_f and the r^2 values between GMD and a_f as enlisted in Table S3 also point out the same. Thus, even though a dip in D_C should

18

correspond with an increase in a_f and vice-versa, this does not usually happen as the change in Dc is less compared to the shift in size distribution such that not only the highest number concentration values changes, the diameter at which this occurs also changes, thereby changing the number available for activation. For example, in Figure 7 two different size distributions for AS air mass at 02:00 and 11:00 have been compared. At 02:00 and 11:00, the following characteristics were noted: (a) $GMD_{02:00}$: 83.78±16.58 nm which is considerably higher than $GMD_{11:00}$: 47.18±13.01 nm, (b) $GSD_{02:00}$: 1.69±0.13 nm which is nearly the same as $GSD_{11:00}$: 1.62±0.14 nm, (c) $D_{C02:00}$: 44.45±3.83 nm which is slightly higher than $D_{C11:00}$: 43.48±2.28 nm (at 0.4% SS), (d) $CN_{02:00}$: 15849±9269 cm^{-3} which is lower than $CN_{11:00}$: 25873±9840 cm^{-3} (e) $CN\_Aitken_{02:00}$: 9819±5945 cm^{-3} which is lower than $CN\_Aitken_{11:00}$: 22376±9693 cm^{-3}, (f) $CN\_Accu_{02:00}$: 5729±3684 cm^{-3} which is higher than $CN\_Accu_{11:00}$: 3311±1569 cm^{-3} (g) $a_{f02:00}$: 0.75±0.12 which is considerably higher than $a_{f11:00}$:0.38± 0.17 at 0.4% SS (h) $CCN_{02:00}$: 11595±6710 cm^{-3} which is higher than $CCN_{11:00}$: 8946±3899 cm^{-3}. The a_f at 02:00 is higher than that at 11:00. D_c decrease should correspond to CCN increase, but the magnitude of ΔD_C = 0.97 nm is very small. The decrease in GMD (ΔGMD = 36.6 nm), on the other hand, is very high with negligible changes in GSD. At 02:00, since D_C is considerably lesser than GSD, most of the particles are counted for activation. At 11:00, since D_C and GMD are very close, nearly 50% of particles are not available for activation. The very high Aitken mode concentration at 11:00 (higher than that at 02:00) is not available for activation at both the times. Thus, N_{CCN} over here is being governed by the accumulation mode which is higher at 02:00, thus making N_{CCN} higher. In this scenario, N_{CCN} and a_f go hand in hand. However, there also exists a second possibility. For e.g., for the SA branch, CCN at 0.4% SS at 08:00 is higher than that at 05:00, while the a_f at 08:00 is lower than that at 05:00 (Figure 6). N_{CCN} is governed at these times by Aitken mode which is higher at 08:00 while a_f is governed by GMD which is lower at 08:00. Thereby, it is clearly established that CCN is governed by CN (dominantly by either, Aitken or Accumulation mode as the case may be), while the a_f is governed by GMD.

At this junction, it would also be pertinent to mention how chemical dispersion and parameters governing CCN are inter-connected. The standard deviation of κ ($\sigma(κ)$) around κ is often used as an estimate of the degree of heterogeneity (chemical dispersion) of particles (Psichoudaki et al., 2018; Lance et al., 2013). The chemical dispersion for all air masses and their sub-branches have been shown in Figures 6, S4 and S5. The chemical dispersion for SA air mass during the early hours (6:00-8:00) coincided with chloride emissions and during the late night after 20:00 with POA and OOA emissions. During the time of high chloride emissions, κ also peaked since inorganics are associated with high hygroscopicity, while during the late hours, κ dropped due to an increase in organics associated with low hygroscopcity. The diurnal patterns of activated fraction, GMD and chemical

19

It is also hereby established that while the physical properties impact CCN directly compared to chemical properties, the physical properties are in turn governed by the chemical properties. The chemical properties impact CCN and a_f indirectly in two ways: (a) the diurnal patterns of $NRPM_1$ species impact the diurnal pattern of Aitken and Accumulation modes which impact CCN and (b) the impact of $NRPM_1$ species on κ, hence D_c and subsequently CCN by impacting the size regime available for activation.

4 Conclusion

Long term measurements of $NRPM_1$ species and size distribution data were carried out at New Delhi. The air masses originated from SA (L, R1, R2, and R3), BB (B and B.reg) and AS. κ was estimated using mixing rule and the bulk κ was assumed for the entire size distribution. Using κ and size distribution data, CCN estimates were obtained. The SA air mass was the most contaminated air-mass followed by BB and then AS. This resulted in higher $NRPM_1$, CN (both Aitken and Accumulation modes), N_{CCN} and a_f for SA > BB > AS. The most dominant salts turned out to be $(NH_4)_2SO_4$ for AS and BB and NH_4Cl for SA. A, B and L branches were completely neutralized while B.reg, R1, R2, and R3 were partially neutralized. The diurnal variations of $NRPM_1$ species were governed by source activities aerosol pre-cursors like SO_x, NO_x, NH_3, O_3, and O_x. The high PM_1 concentration for Delhi which exceeds the National Ambient Air Quality Standards can be mitigated only by controlling both the primary emissions and precursors. In order to address the situation justly, following measures are lacking: a) Data enlisting measurements of PM_1 emissions from various industries in India and Asia, b) Description of the chemical constituents of aerosol that are being emitted, both qualitatively and quantitatively, c) Defining emission limits and complying with the same.

The mean κ ~0.3 was the same for all air-masses, with the diurnal variation of κ being governed by chemical species and thus, source activities. The κ diurnal trends impacted the D_C diurnal trend which in turn affected the available regime for activation. The N_{CCN} diurnal patterns were driven by Accumulation mode at lower SS and Aitken mode with an increase in SS, depending upon D_C which decreases with an increase in SS. The D_C obtained for Delhi was lower than that seen at other places in IGP, for example, Kanpur. The activated fraction for Delhi was very high (0.71±0.15 at 0.4% SS for R1), with the means of activated fractions varying between 0.19-0.87 for SS varying from 0.1-0.8%, whereby its diurnal patterns were governed by GMD. A CCN measurement study with a CCN counter in the future can help verify the estimates, and a closure ratio may be determined. However,

20

in the absence of long-term CCN counter measurements, the importance of these findings cannot be neglected. These results can serve as valuable inputs to GCMs to better quantify precipitation. The high $NRPM_1$ loading and activated fractions are bound to significantly impact precipitation over Delhi, aerosol radiation budget and indirect effects, and need to be investigated thoroughly in the future. These investigations may answer the short intense

5   precipitation events occurring over Delhi and the decrease in the overall rainfall over the past half-century.

10   *Competing interests*. The authors declare that they have no conflict of interest.

References

Andreae, M. O., & Rosenfeld, D.: Aerosol–cloud–precipitation interactions. Part 1. The nature and sources of cloud-active aerosols, Earth-Science Reviews, 89(1-2), 13-41, https://doi.org/10.1016/j.earscirev.2008.03.001,

20   2008.

Asa-Awuku, A., Moore, R. H., Nenes, A., Bahreini, R., Holloway, J. S., Brock, C. A., .,. & Hecobian, A. : Airborne cloud condensation nuclei measurements during the 2006 Texas Air Quality Study, Journal of Geophysical Research: Atmospheres, 116(D11), https://doi.org/10.1029/2010JD014874, 2011.

Bhandari, S., Gani, S., Patel, K., Wang, D., Soni, P., Arub, Z., .,. & Hildebrandt Ruiz, L.: Sources and atmospheric

25   dynamics of organic aerosol in New Delhi, India: Insights from receptor modelling, Atmospheric Physics and Chemistry Discussions, https://doi.org/10.5194/acp-2019-403, 2019.

Bhattu, D., & Tripathi, S. N.: CCN closure study: Effects of aerosol chemical composition and mixing state, Journal of Geophysical Research: Atmospheres, 120(2), 766-783, https://doi.org/10.1002/2014JD021978, 2015.

Bhattu, D., & Tripathi, S. N.: Inter-seasonal variability in size-resolved CCN properties at Kanpur, India, Atmospheric environment, 85, 161-168, https://doi.org/10.1016/j.atmosenv.2013.12.016, 2014.

Bi, X., Zhang, G., Li, L., Wang, X., Li, M., Sheng, G., .,. & Zhou, Z.: Mixing state of biomass burning particles by single particle aerosol mass spectrometer in the urban area of PRD, China, Atmospheric Environment, 45(20), 3447-3453, https://doi.org/10.1016/j.atmosenv.2011.03.034 , 2011.

Boucher, O., Randall, D., Artaxo, P., Bretherton, C., Feingold, G., Forster, P., .,. & Rasch, P.: Clouds and aerosols, In Climate change 2013: the physical science basis. Contribution of Working Group I to the Fifth Assessment Report of the Intergovernmental Panel on Climate Change (pp. 571-657). Cambridge University Press, 2013.

Bougiatioti, A., Fountoukis, C., Kalivitis, N., Pandis, S. N., Nenes, A., & Mihalopoulos, N.: Cloud condensation nuclei measurements in the marine boundary layer of the Eastern Mediterranean: CCN closure and droplet growth kinetics. Atmos. Chem. Phys., 9, 7053–7066, 2009.

Bougiatioti, A., Nenes, A., Fountoukis, C., Kalivitis, N., Pandis, S. N., and Mihalopoulos, N.: Size-resolved CCN distributions and activation kinetics of aged continental and marine aerosol, Atmos. Chem. Phys., 11, 8791-8808, https://doi.org/10.5194/acp-11-8791-2011, 2011.

Braga, R. C., Rosenfeld, D., Weigel, R., Jurkat, T., Andreae, M. O., Wendisch, M., Pöschl, U., Voigt, C., Mahnke, C., Borrmann, S., Albrecht, R. I., Molleker, S., Vila, D. A., Machado, L. A. T., and Grulich, L.: Further evidence for CCN aerosol concentrations determining the height of warm rain and ice initiation in convective clouds over the Amazon basin, Atmos. Chem. Phys., 17, 14433–14456, https://doi.org/10.5194/acp-17-14433-2017, 2017.

Brock, C. A., Wagner, N. L., Anderson, B. E., Beyersdorf, A., Campuzano-Jost, P., Day, D. A., Diskin, G. S., Gordon, T. D., Jimenez, J. L., Lack, D. A., Liao, J., Markovic, M. Z., Middlebrook, A. M., Perring, A. E., Richardson, M. S., Schwarz, J. P., Welti, A., Ziemba, L. D., and Murphy, D. M.: Aerosol optical properties in the southeastern United States in summer – Part 2: Sensitivity of aerosol optical depth to relative humidity and aerosol parameters, Atmos. Chem. Phys., 16, 5009–5019, https://doi.org/10.5194/acp-16-5009-2016, 2016.

Chakraborty, A., Bhattu, D., Gupta, T., Tripathi, S. N., & Canagaratna, M. R.: Real-time measurements of ambient aerosols in a polluted Indian city: Sources, characteristics, and processing of organic aerosols during foggy and nonfoggy periods, Journal of Geophysical Research: Atmospheres, 120(17), 9006-9019, https://doi.org/10.1002/2015JD023419, 2015.

5   Chakraborty, A., Gupta, T., & Tripathi, S. N.: Chemical composition and characteristics of ambient aerosols and rainwater residues during Indian summer monsoon: Insight from aerosol mass spectrometry, Atmospheric environment, 136, 144-155, https://doi.org/10.1016/j.atmosenv.2016.04.024 , 2016.

Chen, Y., Wild, O., Wang, Y., Ran, L., Teich, M., Größ, J., .,. & McFiggans, G.: The influence of impactor size cut-off shift caused by hygroscopic growth on particulate matter loading and composition
10   measurements, Atmospheric environment, 195, 141-148, https://doi.org/10.1016/j.atmosenv.2018.09.049, 2018.

Cheney, J. L., Conner, W. D., Bennett, R. L., Duke, D. L., & Walters, C. L.: Formation of a detached plume from a cement plant, NTIS, SPRINGFIELD, VA(USA), 1983.

Derwent, R. G., Ryall, D. B., Jennings, S. G., Spain, T. G., & Simmonds, P. G.: Black carbon aerosol and carbon monoxide in European regionally polluted air masses at Mace Head, Ireland during 1995–1998, Atmospheric
15   Environment, 35(36), 6371-6378, https://doi.org/10.1016/S1352-2310(01)00394-6, 2001.

Draxler, R. R., & Rolph, G. D.: HYSPLIT (HYbrid Single-Particle Lagrangian Integrated Trajectory) model access via NOAA ARL READY website, NOAA Air Resources Laboratory, Silver Spring, MD, 25, http://ready. arl. noaa. gov/HYSPLIT. php, 2003.

Du, H. H., Kong, L. D., Cheng, T., Chen, J., Yang, X., Zhang, R., .,. & Ma, Y.: Insights into ammonium particle-
20   to-gas conversion: non-sulfate ammonium coupling with nitrate and chloride. Aerosol Air Qual. Res, 10(6), 589-595, https://doi.org/ 10.4209/aaqr.2010.04.0034 , 2010.

Dusek, U., Frank, G. P., Curtius, J., Drewnick, F., Schneider, J., Kürten, A., .,. & Pöschl, U.: Enhanced organic mass fraction and decreased hygroscopicity of cloud condensation nuclei (CCN) during new particle formation events, Geophysical Research Letters, 37(3), https://doi.org/10.1029/2009GL040930, 2010.

25   Engelhart, G. J., Hennigan, C. J., Miracolo, M. A., Robinson, A. L., and Pandis, S. N.: Cloud condensation nuclei activity of fresh primary and aged biomass burning aerosol, Atmos. Chem. Phys., 12, 7285-7293, https://doi.org/10.5194/acp-12-7285-2012, 2012.

Erickson, R. E., Yates, L. M., Clark, R. L., & McEwen, D.: The reaction of sulfur dioxide with ozone in water and its possible atmospheric significance, Atmospheric Environment (1967), 11(9), 813-817, https://doi.org/10.1016/0004-6981(77)90043-9, 1977.

Ervens, B., Turpin, B. J., and Weber, R. J.: Secondary organic aerosol formation in cloud droplets and aqueous
5   particles (aqSOA): a review of laboratory, field and model studies, Atmos. Chem. Phys., 11, 11069-11102, https://doi.org/10.5194/acp-11-11069-2011, 2011.

Esri, Garmin International, 2010: World Countries (Generalized), https://www.arcgis.com/home/item.html?id=170b5e6529064b8d9275168687880359, 2010.

Fuzzi, S., Decesari, S., Facchini, M. C., Cavalli, F., Emblico, L., Mircea, M., .,. & Artaxo, P.: Overview of the
10   inorganic and organic composition of size-segregated aerosol in Rondonia, Brazil, from the biomass-burning period to the onset of the wet season, Journal of Geophysical Research: Atmospheres, 112(D1), https://doi.org/10.1029/2005JD006741, 2007.

Gandhi, H. S., & Shelef, M.: Effects of sulphur on noble metal automotive catalysts, *Applied Catalysis*, *77*(2), 175-186, https://doi.org/10.1016/0166-9834(91)80063-3, 1991.

15   Gani, S., Bhandari, S., Seraj, S., Wang, D. S., Patel, K., Soni, P., Arub, Z., Habib, G., Hildebrandt Ruiz, L., and Apte, J. S.: Submicron aerosol composition in the world's most polluted megacity: the Delhi Aerosol Supersite study, Atmos. Chem. Phys., 19, 6843–6859, https://doi.org/10.5194/acp-19-6843-2019, 2019.

Gaur, A., Tripathi, S. N., Kanawade, V. P., Tare, V., & Shukla, S. P.: Four-year measurements of trace gases (SO 2, NO x, CO, and O 3) at an urban location, Kanpur, in Northern India, Journal of Atmospheric Chemistry, *71*(4),
20   283-301, https://doi.org/10.1007/s10874-014-9295-8, 2014.

Guhathakurta, P., Rajeevan, M., Sikka, D. R., & Tyagi, A.: Observed changes in southwest monsoon rainfall over India during 1901–2011, International Journal of Climatology, *35*(8), 1881-1898, https://doi.org/10.1002/joc.4095, 2015.

Gunn, R., & Phillips, B. B.: An experimental investigation of the effect of air pollution on the initiation of
25   rain, Journal of Meteorology, 14(3), 272-280, https://doi.org/10.1175/1520-0469(1957)014<0272:AEIOTE>2.0.CO;2 , 1957.

24

Gunthe, S. S., Rose, D., Su, H., Garland, R. M., Achtert, P., Nowak, A., .,. & Hu, M.: Cloud condensation nuclei (CCN) from fresh and aged air pollution in the megacity region of Beijing, Atmospheric Chemistry and Physics, 11(21), 11023-11039, https://doi/10.5194/acp-11-11023-2011, 2011.

Gunthe, S. S., King, S. M., Rose, D., Chen, Q., Roldin, P., Farmer, D. K., .,. & Pöschl, U.: Cloud condensation nuclei in pristine tropical rainforest air of Amazonia: size-resolved measurements and modeling of atmospheric aerosol composition and CCN activity, Atmospheric Chemistry and Physics, 9(19), 7551-7575, 2009.

Habib, G., Venkataraman, C., Chiapello, I., Ramachandran, S., Boucher, O., & Reddy, M. S.: Seasonal and interannual variability in absorbing aerosols over India derived from TOMS: Relationship to regional meteorology and emissions, Atmospheric Environment, 40(11), 1909-1921, https://doi.org/10.1016/j.atmosenv.2005.07.077, 2006.

Harrison, R. M., & Pio, C. A.: Major ion composition and chemical associations of inorganic atmospheric aerosols, Environmental science & technology, 17(3), 169-174, https://doi.org/10.1021/es00109a009, 1983.

Haynes, W. M.: CRC handbook of chemistry and physics, 95th edition. CRC press, 2014.

Ho, K. F., Lee, S. C., Guo, H., & Tsai, W. Y.: Seasonal and diurnal variations of volatile organic compounds (VOCs) in the atmosphere of Hong Kong, Science of the Total Environment, 322(1-3), 155-166, https://doi.org/10.1016/j.scitotenv.2003.10.004, 2004.

Hong, J., Häkkinen, S. A. K., Paramonov, M., Äijälä, M., Hakala, J., Nieminen, T., ... & Bilde, M.: Hygroscopicity, CCN and volatility properties of submicron atmospheric aerosol in a boreal forest environment during the summer of 2010. Atmospheric Chemistry & Physics, 14, 4733–4748, https//doi.org/10.5194/acp-14-4733-2014, 2014.

Jaiprakash, Singhai, A., Habib, G., Raman, R. S., & Gupta, T.: Chemical characterization of PM 1.0 aerosol in Delhi and source apportionment using positive matrix factorization, Environmental Science and Pollution Research, 24(1), 445-462, https://doi.org/10.1007/s11356-016-7708-8, 2017.

Kalapureddy, M. C. R., Kaskaoutis, D. G., Ernest Raj, P., Devara, P. C. S., Kambezidis, H. D., Kosmopoulos, P. G., & Nastos, P. T.: Identification of aerosol type over the Arabian Sea in the premonsoon season during the

Integrated Campaign for Aerosols, Gases and Radiation Budget (ICARB), Journal of Geophysical Research: Atmospheres, 114(D17), https://doi.org/10.1029/2009JD011826, 2009.

Kaneyasu, N., Yoshikado, H., Mizuno, T., Sakamoto, K., & Soufuku, M.: Chemical forms and sources of extremely high nitrate and chloride in winter aerosol pollution in the Kanto Plain of Japan, Atmospheric Environment, 33(11), 1745-1756, https://doi.org/10.1016/S1352-2310(98)00396-3, 1999.

Lance, S., Raatikainen, T., Onasch, T. B., Worsnop, D. R., Yu, X.-Y., Alexander, M.L., Stolzenburg, M. R., McMurry, P. H., Smith, J. N., and Nenes, A.: Aerosol mixing state, hygroscopic growth and cloud activation efficiency during MIRAGE 2006, Atmos. Chem. Phys., 13, 5049–5062, https://doi.org/10.5194/acp-13-5049-2013, 2013.

Lee, S. Y., Gan, C., & Chew, B. N.: Visibility deterioration and hygroscopic growth of biomass burning aerosols over a tropical coastal city: a case study over Singapore's airport, Atmospheric Science Letters, 17(12), 624-629, https://doi.org/10.1002/asl.712, 2016.

Leena, P. P., Pandithurai, G., Anilkumar, V., Murugavel, P., Sonbawne, S. M., & Dani, K. K.: Seasonal variability in aerosol, CCN and their relationship observed at a high altitude site in Western Ghats, Meteorology and Atmospheric Physics, 128(2), 143-153, https://doi.org/10.1007/s00703-015-0406-0, 2016.

Leng, C., Zhang, Q., Tao, J., Zhang, H., Zhang, D., Xu, C., ... & Yang, X.: Impacts of new particle formation on aerosol cloud condensation nuclei (CCN) activity in Shanghai: case study. Atmos. Chem. Phys, 14(20), 11353-11365, https//doi.org/10.5194/acp-14-12499-2014, 2014.

Liu, X., Zhang, Y., Cheng, Y., Hu, M., & Han, T.: Aerosol hygroscopicity and its impact on atmospheric visibility and radiative forcing in Guangzhou during the 2006 PRIDE-PRD campaign, Atmospheric Environment, 60, 59-67, https://doi.org/10.1016/j.atmosenv.2012.06.016, 2012.

Moorthy, K. K., Satheesh, S. K., Babu, S. S., & Dutt, C. B. S.: Integrated campaign for aerosols, gases and radiation budget (ICARB): an overview, Journal of Earth System Science, 117(1), 243-262, https://doi.org/10.1007/s12040-008-0029-7, 2008.

Nair, V. S., Moorthy, K. K., Babu, S. S., Narasimhulu, K., Reddy, L. S. S., Reddy, R. R., .,. & Niranjan, K.: Size segregated aerosol mass concentration measurements over the Arabian Sea during ICARB, Journal of earth system science, 117(1), 315-323, https://doi.org/10.1007/s12040-008-0034-x, 2008a.

Nair, V. S., Babu, S. S., & Moorthy, K. K.: Aerosol characteristics in the marine atmospheric boundary layer over the Bay of Bengal and Arabian Sea during ICARB: Spatial distribution and latitudinal and longitudinal gradients, Journal of Geophysical Research: Atmospheres, 113(D15), https://doi.org/10.1029/2008JD009823, 2008b.

5   Nenes, A., Pandis, S. N., & Pilinis, C.: ISORROPIA: A new thermodynamic equilibrium model for multiphase multicomponent inorganic aerosols, Aquatic geochemistry, 4(1), 123-152, https://doi.org/10.1023/A:1009604003981, 1998.

Ng, N. L., Canagaratna, M. R., Jimenez, J. L., Zhang, Q., Ulbrich, I. M., & Worsnop, D. R.: Real-time methods for estimating organic component mass concentrations from aerosol mass spectrometer data, Environmental
10   science & technology, 45(3), 910-916, https://doi.org/10.1021/es102951k, 2010.

Padró, L. T., Moore, R. H., Zhang, X., Rastogi, N., Weber, R. J., and Nenes, A.: Mixing state and compositional effects on CCN activity and droplet growth kinetics of size-resolved CCN in an urban environment, Atmos. Chem. Phys., 12, 10239-10255, https://doi.org/10.5194/acp-12-10239-2012, 2012.

Pan, Y., Tian, S., Liu, D., Fang, Y., Zhu, X., Zhang, Q., .,. & Wang, Y.: Fossil fuel combustion-related emissions
15   dominate atmospheric ammonia sources during severe haze episodes: Evidence from 15N-stable isotope in size-resolved aerosol ammonium, Environmental science & technology, 50(15), 8049-8056, https://doi.org/10.1021/acs.est.6b00634, 2016.

Petters, M. D., & Kreidenweis, S. M.: A single parameter representation of hygroscopic growth and cloud condensation nucleus activity, Atmospheric Chemistry and Physics, 7(8), 1961-1971, 2007.

20   Petters, M. D., Carrico, C. M., Kreidenweis, S. M., Prenni, A. J., DeMott, P. J., Collett Jr, J. L., & Moosmüller, H.: Cloud condensation nucleation activity of biomass burning aerosol. Journal of Geophysical Research: Atmospheres, 114(D22), https://doi.org/10.1029/2009JD012353, 2009.

Pöschl, U., Rose, D., & Andreae, M. O.: Climatologies of Cloud-Related Aerosols—Part 2: Particle Hygroscopicity and Cloud Condensation Nucleus Activity. Clouds in the Perturbed Climate System: Their
25   Relationship to Energy Balance, Atmospheric Dynamics, and Precipitation, 58-72, 2009.

Pringle, K. J., Tost, H., Pozzer, A., Pöschl, U., and Lelieveld, J.: Global distribution of the effective aerosol hygroscopicity parameter for CCN activation, Atmos. Chem. Phys., 10, 5241-5255, https://doi.org/10.5194/acp-10-5241-2010, 2010.

Psichoudaki, M., Nenes, A., Florou, K., Kaltsonoudis, C., & Pandis, S. N.: Hygroscopic properties of atmospheric particles emitted during wintertime biomass burning episodes in Athens. Atmospheric Environment, 178, 66–72, doi:10.1016/j.atmosenv.2018.01.004, 2018.

Rajput, P., Mandaria, A., Kachawa, L., Singh, D. K., Singh, A. K., & Gupta, T.: Wintertime source-apportionment of PM1 from Kanpur in the Indo-Gangetic plain, Clim Change, 1(4), 503-507, 2015.

Ram, K., Tripathi, S. N., Sarin, M. M., & Bhattu, D.: Primary and secondary aerosols from an urban site (Kanpur) in the Indo-Gangetic Plain: impact on CCN, CN concentrations and optical properties, Atmospheric Environment, 89, 655-663, https://doi.org/10.1016/j.atmosenv.2014.02.009, 2014.

Reddy, M. S., & Venkataraman, C.: Inventory of aerosol and sulphur dioxide emissions from India: I—Fossil fuel combustion, Atmospheric Environment, 36(4), 677-697, https://doi.org/10.1016/S1352-2310(01)00463-0 , 2002.

Rissler, J., Swietlicki, E., Zhou, J., Roberts, G., Andreae, M. O., Gatti, L. V., & Artaxo, P.: Physical properties of the sub-micrometer aerosol over the Amazon rain forest during the wet-to-dry season transition-comparison of modeled and measured CCN concentrations, Atmospheric Chemistry and Physics, 4(8), 2119-2143, https://doi.org/10.5194/acp-4-2119-2004, 2004.

Rose, D., Nowak, A., Achtert, P., Wiedensohler, A., Hu, M., Shao, M., Zhang, Y., Andreae, M. O., and Pöschl, U.: Cloud condensation nuclei in polluted air and biomass burning smoke near the mega-city Guangzhou, China – Part 1: Size-resolved measurements and implications for the modeling of aerosol particle hygroscopicity and CCN activity, Atmos. Chem. Phys., 10, 3365-3383, https://doi.org/10.5194/acp-10-3365-2010, 2010.

Rose, D., Gunthe, S. S., Su, H., Garland, R. M., Yang, H., Berghof, M., Cheng, Y. F., Wehner, B., Achtert, P., Nowak, A., Wiedensohler, A., Takegawa, N., Kondo, Y., Hu, M., Zhang, Y., Andreae, M. O., and Pöschl, U.: Cloud condensation nuclei in polluted air and biomass burning smoke near the mega-city Guangzhou, China –

Part 2: Size-resolved aerosol chemical composition, diurnal cycles, and externally mixed weakly CCN-active soot particles, Atmos. Chem. Phys., 11, 2817-2836, https://doi.org/10.5194/acp-11-2817-2011, 2011.

Rosenfeld, D., Lohmann, U., Raga, G. B., O'Dowd, C. D., Kulmala, M., Fuzzi, S., .,. & Andreae, M. O.: Flood or drought: how do aerosols affect precipitation?, Science, 321(5894), 1309-1313, https//doi.org/ 10.1126/science.1160606, 2008.

Rosenfeld, D., Lahav, R., Khain, A., & Pinsky, M.: The role of sea spray in cleansing air pollution over ocean via cloud processes, Science, 297(5587), 1667-1670, https//doi.org/10.1126/science.1073869, 2002.

Rosenfeld, D.: Suppression of rain and snow by urban and industrial air pollution. Science, 287(5459), 1793-1796, https//doi.org/10.1126/science.287.5459.1793, 2000.

Rosenfeld, D.: TRMM observed first direct evidence of smoke from forest fires inhibiting rainfall, Geophysical research letters, 26(20), 3105-3108, https://doi.org/10.1029/1999GL006066, 1999.

Roy, A., Chatterjee, A., Sarkar, C., Das, S. K., Ghosh, S. K., & Raha, S.: A study on aerosol-cloud condensation nuclei (CCN) activation over eastern Himalaya in India, Atmospheric research, 189, 69-81, https://doi.org/10.1016/j.atmosres.2017.01.015, 2017.

Rudich, Y., Khersonsky, O., & Rosenfeld, D.:Treating clouds with a grain of salt, Geophysical Research Letters, 29(22), 17-1, https://doi.org/10.1029/2002GL016055, 2002.

Seinfeld, J. H.: Atmospheric Chemistry and Physics of Air Pollution, Environmental science & technology, 20(9), 863-863, https://doi.org/10.1021/es00151a602, 1986.

Sharma, S. K., Kumar, M., Gupta, N. C., Saxena, M., & Mandal, T. K.: Characteristics of ambient ammonia over Delhi, India, Meteorology and Atmospheric Physics, 124(1-2), 67-82, https://doi.org/10.1007/s00703-013-0299-8, 2014.

Jaiprakash, Singhai, A., Habib, G., Raman, R. S., & Gupta, T.: Chemical characterization of PM 1.0 aerosol in Delhi and source apportionment using positive matrix factorization, Environmental Science and Pollution Research, 24(1), 445-462, https://doi.org/10.1007/s11356-016-7708-8, 2017.

Sodeman, D. A., Toner, S. M., & Prather, K. A.: Determination of single particle mass spectral signatures from light-duty vehicle emissions, Environmental Science & Technology, 39(12), 4569-4580, https://doi.org/10.1021/es0489947, 2005.

Squires, P.:The microstructure and colloidal stability of warm clouds: Part II—The causes of the variations in
5   microstructure, Tellus, 10(2), 262-271, https://doi.org/10.1111/j.2153-3490.1958.tb02012.x, 1958.

Stelson, A. W., & Seinfeld, J. H.: Relative humidity and pH dependence of the vapor pressure of ammonium nitrate-nitric acid solutions at 25 C, Atmospheric Environment (1967), 16(5), 993-1000, https://doi.org/10.1016/0004-6981(82)90185-8, 1982.

Sullivan, R.C., Moore, M.J.K., Petters, M.D., Kreidenweis, S.M., Roberts, G.C., Prather, K.A.: Effect of chemical
10 mixing state on the hygroscopicity and cloud nucleation properties of calcium mineral dust particles. Atmos. Chem. Phys., 9, 3303–3316, https://doi.org/10.5194/acp-9-3303-2009, 2009.

Tao, W. K., Chen, J. P., Li, Z., Wang, C., & Zhang, C.: Impact of aerosols on convective clouds and precipitation, Reviews of Geophysics, 50(2), https://doi.org/10.1029/2011RG000369, 2012.

Tiwari, S., Dahiya, A., & Kumar, N.: Investigation into relationships among NO, NO2, NOx, O3, and CO at an
15 urban background site in Delhi, India, Atmospheric Research, 157, 119-126, https://doi.org/10.1016/j.atmosres.2015.01.008, 2015.

Turšič, J., Podkrajšek, B., Grgić, I., Ctyroky, P., Berner, A., Dusek, U., & Hitzenberger, R.: Chemical composition and hygroscopic properties of size-segregated aerosol particles collected at the Adriatic coast of Slovenia, Chemosphere, 63(7), 1193-1202, https://doi.org/10.1016/j.chemosphere.2005.08.040, 2006.

20 Wang, J., Cubison, M. J., Aiken, A. C., Jimenez, J. L., & Collins, D. R.: The importance of aerosol mixing state and size-resolved composition on CCN concentration and the variation of the importance with atmospheric aging of aerosols, Atmospheric Chemistry and Physics, 10(15), 7267-7283, https://doi.org/10.5194/acp-10-7267-2010, 2010.

Wang, J., & Martin, S. T.: Satellite characterization of urban aerosols: Importance of including hygroscopicity
25 and mixing state in the retrieval algorithms, Journal of Geophysical Research: Atmospheres, 112(D17), https://doi.org/10.1029/2006JD008078, 2007.

Wang, S., Nan, J., Shi, C., Fu, Q., Gao, S., Wang, D., .,. & Zhou, B.: Atmospheric ammonia and its impacts on regional air quality over the megacity of Shanghai, China, Scientific reports, 5, 15842, https://doi.org/10.1038/srep15842, 2015.

Wang, Y., & Chen, Y.: Significant Climate Impact of Highly Hygroscopic Atmospheric Aerosols in Delhi, India,
5   Geophysical Research Letters, https://doi.org/10.1029/2019GL082339, 2019.

Wu, Z. J., Poulain, L., Henning, S., Dieckmann, K., Birmili, W., Merkel, M., ... & H Herrmann, H.: Relating particle hygroscopicity and CCN activity to chemical composition during the HCCT-2010 field campaign. Atmos. Chem. Phys, 13, 7983–7996, https//doi.org/10.5194/acp-13-7983-2013, 2013.

Zhang, Q., Jimenez, J. L., Worsnop, D. R., & Canagaratna, M.: A case study of urban particle acidity and its
10   influence on secondary organic aerosol, Environmental science & technology, 41(9), 3213-3219, https://doi.org/10.1021/es061812j, 2007.

List of figures

Figure 1: HYSPLIT grouping of cluster mean trajectories based on directions and distances of source regions.
Figure 2: Mean values of (a) $NRPM_1$, (b) Organics, inorganics, and BC, and (c) $NRPM_1$ species' for the various
15   air masses.
Figure 3: Diurnal variation of $NRPM_1$ species (NH_4^+, Cl^-, NO_3^-, SO_4^{2-}, POA, and OOA) and BC for AS to the left, BB (B and B.reg) in the middle and SA (L, R1, R2, and R3) air-masses to the right.SA (L, R1, R2, and R3), BB (B and B.reg) and AS air-masses.
Figure 4: Diurnal variation of κ with time. The graph on the left is for AS, BB and SA, the middle for BB branches
20   (B and B.reg), and the right is for SA branches (L, R1, R2, and R3).
Figure 5: Variation of CCN and activated fraction with SS for AS, BB, and SA air masses.
Figure 6: Diurnal variation of (a) N_{CCN} at 0.1%, 0.4% and 0.8% SS, (b) a_f at 0.1%, 0.4% and 0.8% SS, (c) N_{CN}, N_{Aitken}, $N_{Accumulation,}$ (d) D_c at 0.1%, 0.4% and 0.8% SS, and (e) GMD for AS, BB and SA air masses.
Figure7: Comparing two size different profiles at different times of day for AS branch.
25   Figure S1: HYSPLIT 5-day back trajectory cluster analysis for all seasons
Figure S2: Diurnal variations of volume fractions of $(NH_4)_2SO_4$, NH_4NO_3, NH_4Cl (representing the dominant contributors to hygroscopicity of air masses) and organics.

15 **List of tables**

Figure 1: HYSPLIT grouping of cluster mean trajectories based on directions and distances of source regions. Cluster mean trajectories were obtained for all seasons and clubbed as per directions. AS branch originated from the Arabian Sea, BB branch with sub-branches B and B.reg originated from Bay of Bengal and SA branch with sub-branches L, R1, R2 and R3 from the north-west direction originated mainly in the South Asian landmass. The map layer used is from "World Countries (Generalized)", by Esri, Garmin International, 2010. (https://www.arcgis.com/home/item.html?id=170b5e6529064b8d9275168687880359). Copyright by Esri, Garmin. All rights reserved. This map is an intellectual property of Esri, Garmin and used under license. Further details may be found on www.esri.com.
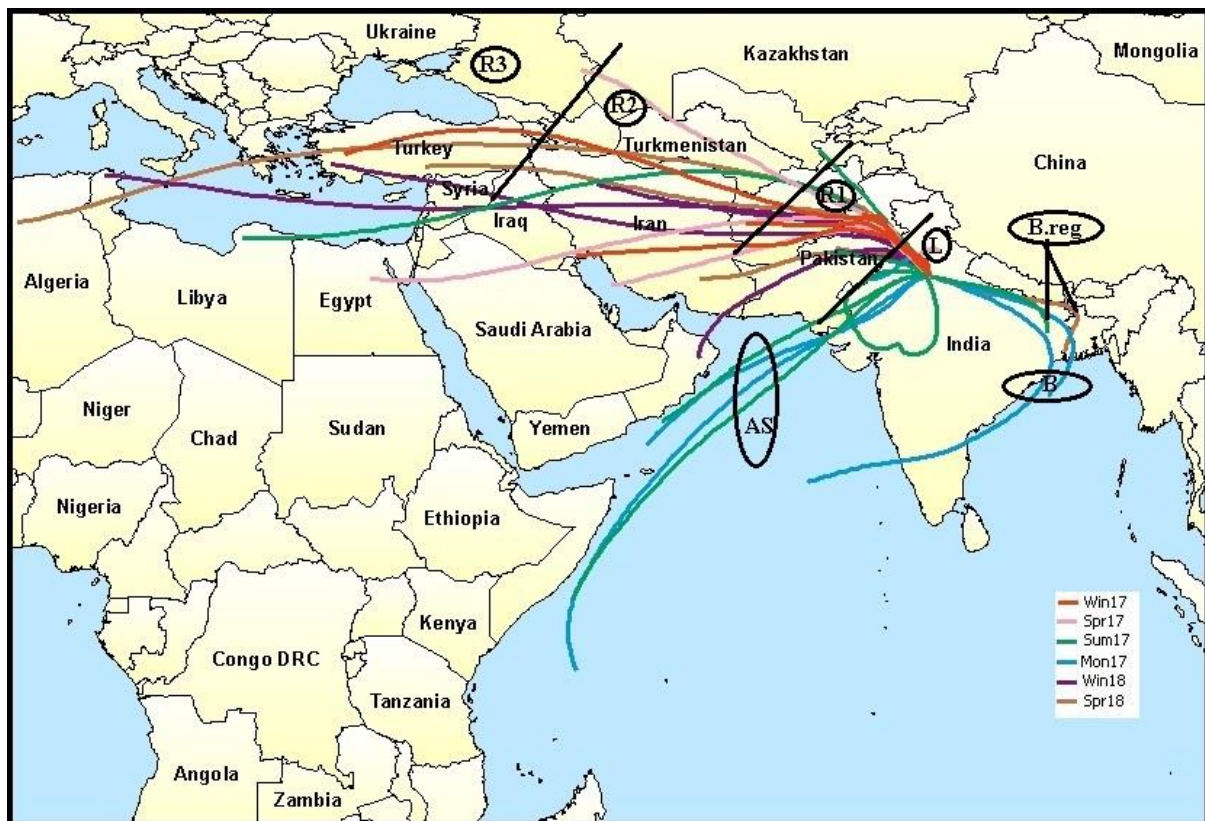
Figure 2: Mean values of (a) NRPM$_1$, (b) Organics, inorganics and BC, and (c) NRPM$_1$ species (from top to bottom) for the various air masses. The graphs on the left are for AS, BB and SA, the middle for BB branches (B and B.reg), and the right for SA branches (L, R1, R2, and R3).

5
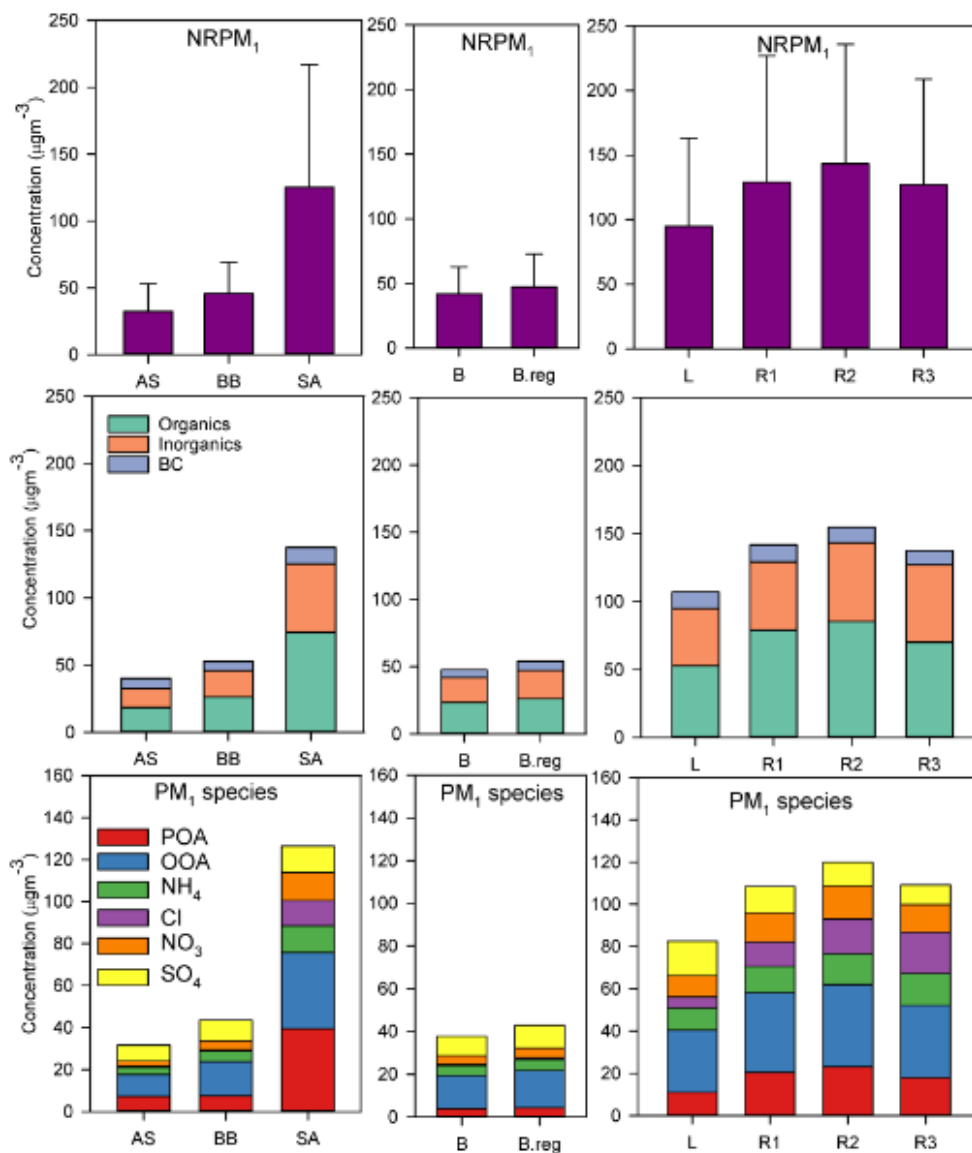
Figure 3: Diurnal variation of NRPM$_1$ species (NH$_4^+$, Cl$^-$, NO$_3^-$, SO$_4^{2-}$, POA, and OOA) and BC for AS SA (L, R1, R2, and R3) to the left, BB (B and B.reg) in the middle and AS SA (L, R1, R2, and R3) air-masses to the right..
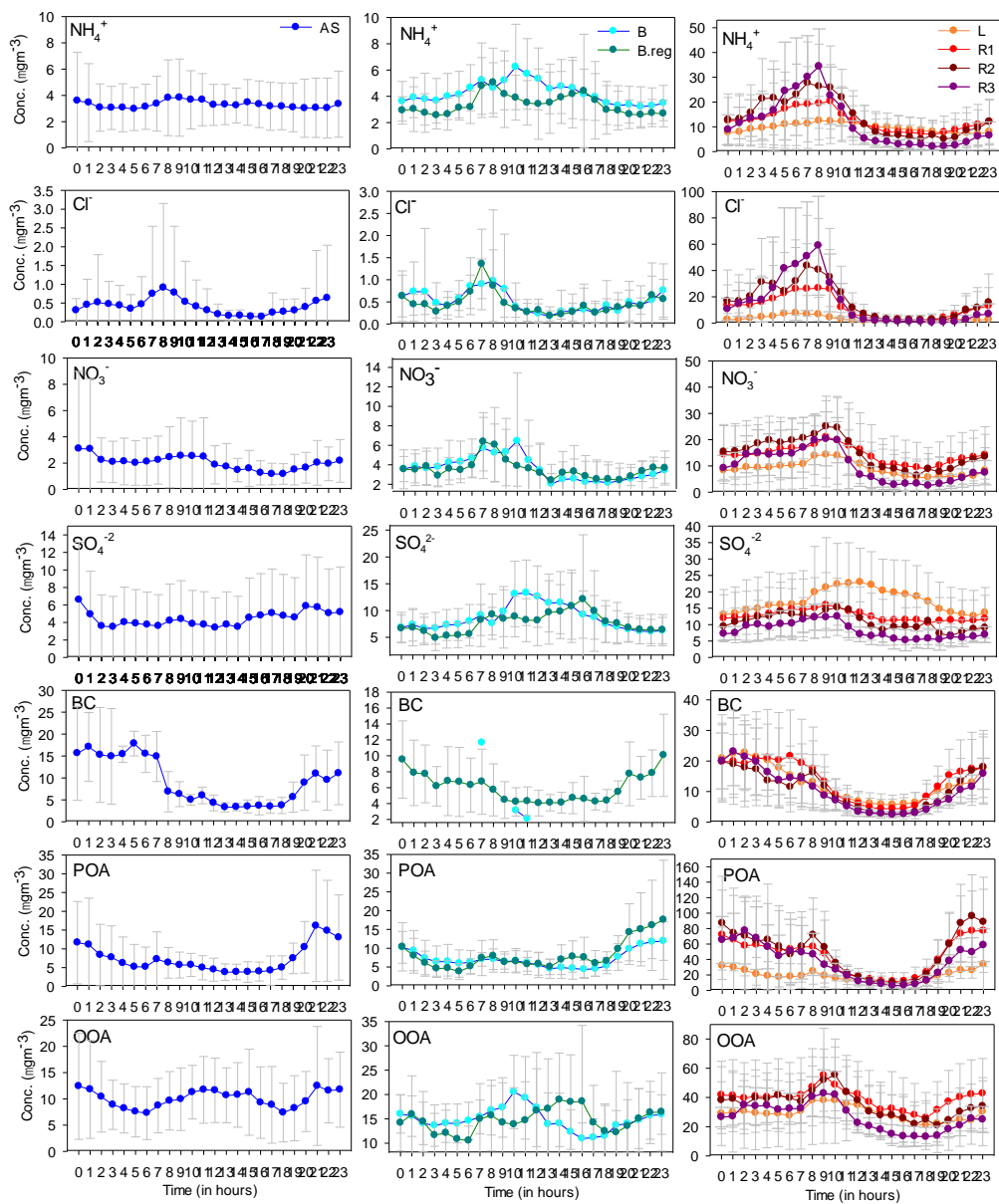
35

Figure 4: Diurnal variation of κ with time. The graph on the left is for AS, BB and SA, the middle for SA branches (L, R1, R2, and R3) and right is for BB branches (B and B.reg), and the right is for SA branches (L, R1, R2, and R3).
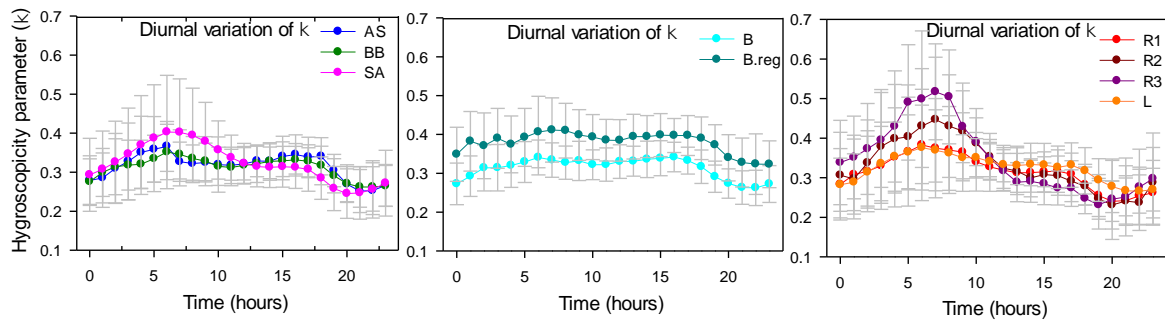
Figure 5: Variation of CCN and activated fraction with SS (%) for AS, BB, and SA air masses.
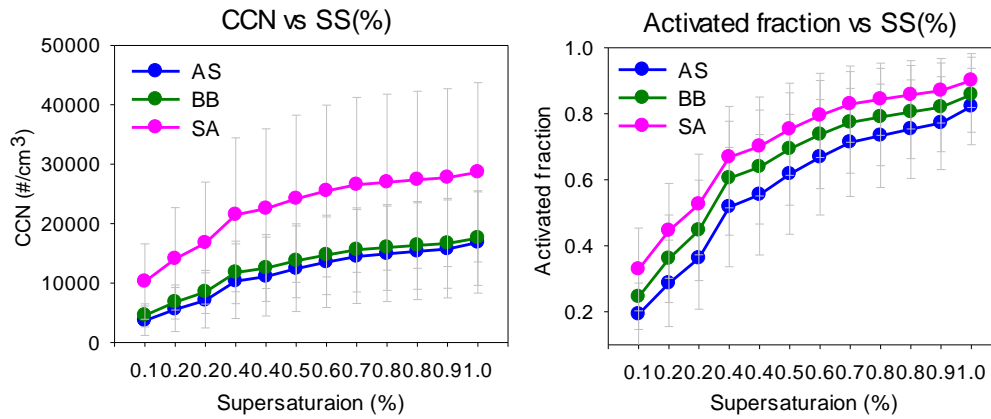
5

10

15

Figure 6: Diurnal variation of (a) N_{CCN} at 0.1%, 0.4% and 0.8% SS, (b) a_f at 0.1%, 0.4% and 0.8% SS, (c) N_{CN} , N_{Aitken} and $N_{Accumulation}$, (d) D_c at 0.1%, 0.4% and 0.8% SS (e) Chemical dispersion, and (f) GMD for AS, BB and SA air masses.

5

Figure7: Comparing two size distribution profiles at different times of day for AS branch at 02:00 and 08:00.

5

10

Table 1: Mean values of NRPM$_1$ species and BC (μg m^{-3}) for all clusters.

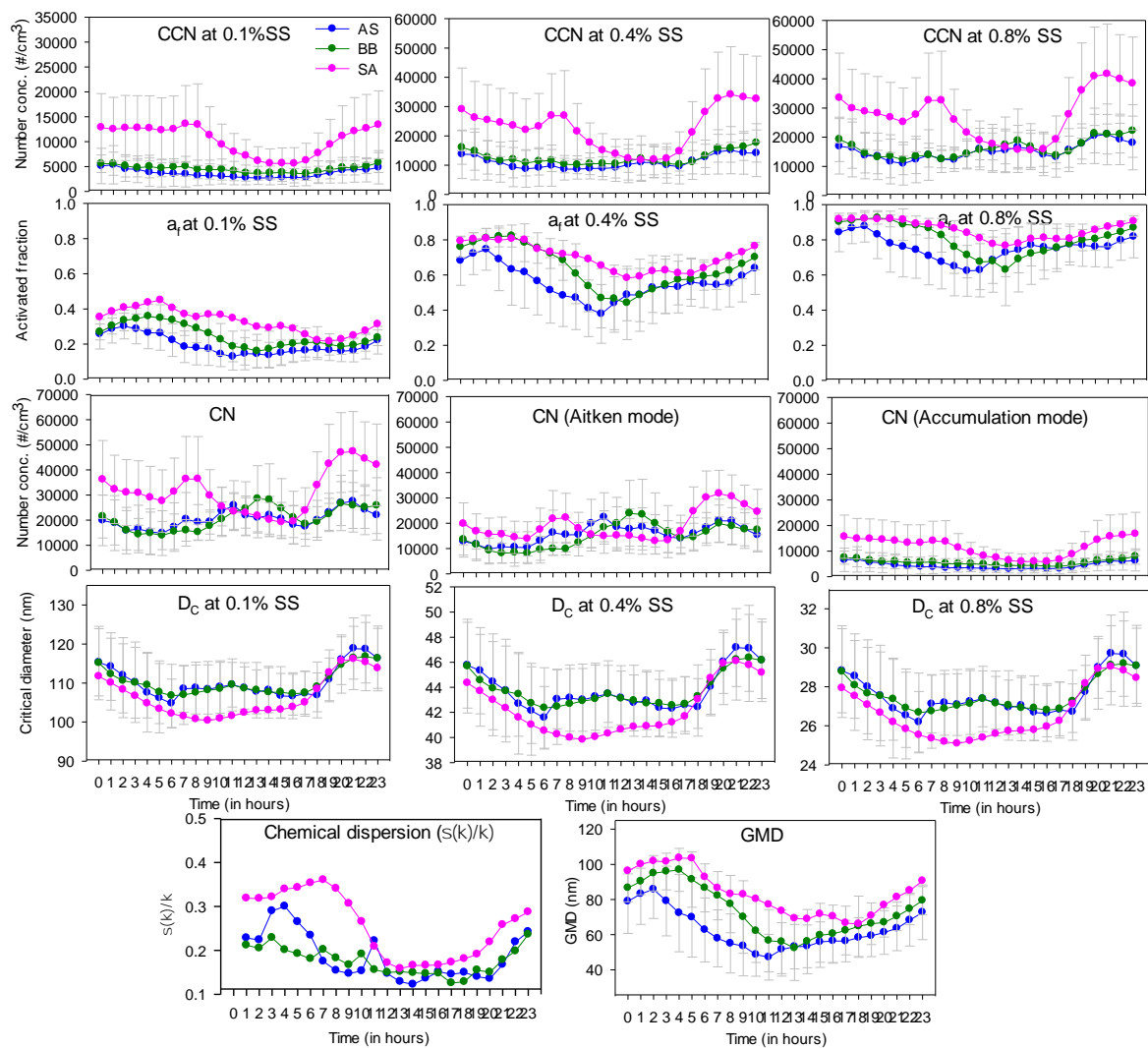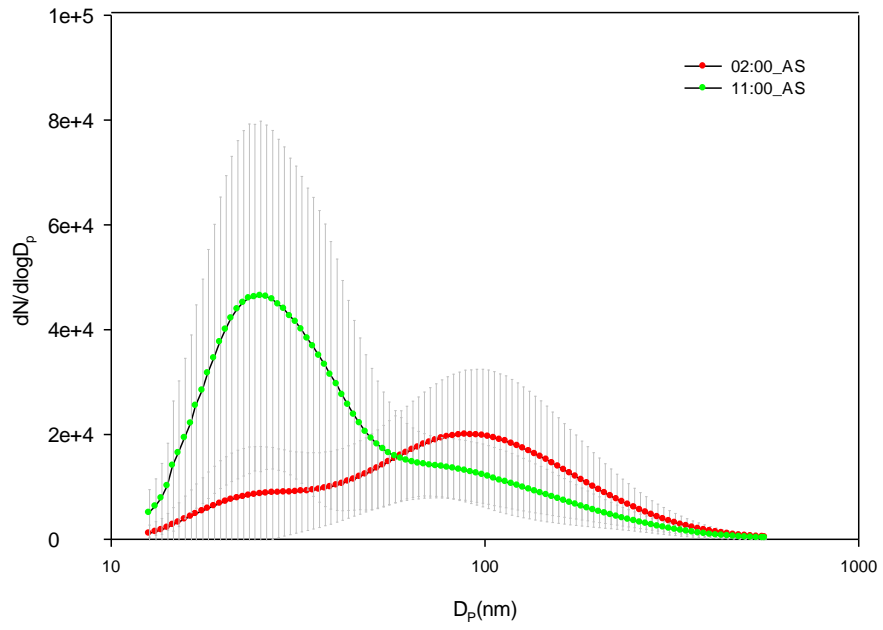| Cluster	NRPM$_1$	BC	NH$_4^+$	Cl$^-$	NO$_3^-$	SO$_4^{2-}$	Inorg	POA	OOA	Org
A	32.5±20.6	7.7±7.6	3.6±2.5	0.5±1.4	2.3±2.9	7.6±4.6	14.0±9.3	7.4±8.1	10.3±7.0	18.5±13.6
BB	45.9±23.4	6.8±5.1	4.8±3.2	0.6±1.1	4.3±3.8	9.9±6.5	19.7±12.4	7.6±5.4	16.3±7.8	26.2±14.1
SA	125.2±91.6	12.1±10.7	12.7±11.1	12.1±20.4	13.3±11.8	12.7±9.7	50.8±44.0	39.5±43.7	36.3±24.2	74.4±58.1
B	41.9±20.7	5.6±5.2	4.6±2.6	0.5±0.7	4.2±3.8	9.1±5.7	18.5±11.0	7.2±4.3	15.5±7.3	23.4±11.5
B.reg	47.350.7±25.4	6.8±5.1	5.2±3.8	0.8±1.4	4.5±3.8	10.7±7.3	21.111.6±3.4	8.5±7.2	17.4±8.4	269.26±16.2
L	94.9±68.1	12.2±9.8	10.,4±8.2	5.2±12.2	10.1±9.7	16.4±9.8	42.0±33.0	18.9±23.1	29.5±21.7	52.9±40.6
R1	129.1±97.6	12.6±11.3	12.3±10.9	11.6±19.4	13.7±12.6	12.5±7.6	50.2±44.2	44.2±46.7	37.7±26	79.0±6.32
R2	143.2±92.5	11.4±10.3	14.6±12.2	16.4±23.6	15.6±11.7	11.3±6.7	57.9±47.5	49.4±49.5	38.9±22.4	85.4±59.9
R3	127.1±81.6	10.4±8.7	15.0±13.4	19.6±26	13.1±10.0	9.3±4.8	56.9±49.7	35.7±31.8	34.3±18.4	70.2±14.7

5

10

Table 2: Cluster means of f57 and f60 values for all branches, where 'Stdev' implies standard deviation.

Cluster	f57 Mean	Stdev	f60 Mean	Stdev
A	0.02389	0.00777	0.004061	0.001199
BB	0.0205	0.006107	0.004294	0.000962
SA	0.02499	0.007663	0.007089	0.003569
B	0.02088	0.005959	0.004368	0.000916
B.reg	0.01998	0.006266	0.004192	0.001012
L	0.0239	0.007179	0.006023	0.002404
R1	0.0254	0.007878	0.00717	0.003861
R2	0.02509	0.00764	0.007851	0.003576
R3	0.02427	0.006971	0.007084	0.002992

5

10

Table 3: Mean values of CCN number concentrations (cm^{-3}) at 0.1%, 0.4% and 0.8% SS for all clusters.

Cluster	CCN at 0.1% SS		CCN at 0.4% SS		CCN at 0.8% SS	
	Mean	Std	Mean	Std	Mean	Std
A	3669	2480	11089	6650	15339	8149
BB	4558	1945	12526	5626	16329	7385
SA	10245	6352	22526	13439	27374	14902
B	4469	1885	11699	4900	14892	5883
B.reg	4726	2043	14088	6506	19040	8993
L	8200	4612	18810	9434	23161	10845
R1	10921	6843	24053	14743	28914	16265
R2	11318	6071	23736	13739	28926	15111
R3	9555	6077	20469	10580	25971	11963

5

10

Table 4: Mean activated fractions at 0.1%, 0.4% and 0.8% SS for all clusters.

Cluster	a_f at 0.1%SS		a_f at 0.4%SS		a_f at 0.8%SS	
	Mean	Std	Mean	Std	Mean	Std
A	0.19	0.09	0.55	0.18	0.75	0.15
BB	0.25	0.10	0.64	0.17	0.81	0.14
SA	0.33	0.13	0.70	0.15	0.86	0.10
B	0.25	0.10	0.65	0.18	0.81	0.15
B.reg	0.23	0.10	0.62	0.16	0.80	0.12
L	0.31	0.11	0.69	0.13	0.85	0.09
R1	0.34	0.13	0.71	0.15	0.87	0.10
R2	0.35	0.13	0.69	0.16	0.85	0.11
R3	0.30	0.13	0.65	0.16	0.82	0.12

5